SORPTION AND TRANSPORT OF WATER VAPOUR IN ACRYLIC PAINTS

by

Özge TOPÇUOĞLU

A Thesis Submitted to the Graduate School of Engineering and Sciences of İzmir Institute of Technology in Partial Fulfillment of the Requirements for the Degree of

MASTER OF SCIENCE

Department: Chemical Engineering

Major: Chemical Engineering

İzmir Institute of Technology

İzmir, Turkey

October 2004

We approve the thesis of **Özge TOPÇUOĞLU**

Date of Signature

..... **27.10.2004**

Assoc. Prof. Sacide ALSOY ALTINKAYA

Supervisor

Department of Chemical Engineering

..... **27.10.2004**

Prof. Devrim BALKÖSE

Co-Supervisor

Department of Chemical Engineering

..... **27.10.2004**

Asst. Prof. Fehime ÖZKAN

Department of Chemical Engineering

..... **27. 10.2004**

Assoc. Prof. Funda TIHMINLIOĞLU

Department of Chemical Engineering

..... **27. 10. 2004**

Assoc. Prof. Metin TANOĞLU

Department of Mechanical Engineering

..... **27.10.2004**

Prof. Devrim BALKÖSE

Head of the Department

ACKNOWLEDGEMENTS

I am deeply grateful to my advisors Assoc. Prof. Sacide Alsoy Altınkaya and Prof. Devrim Balköse for their great support.

Thanks to Yılmaz Yürekli and Burcu Alp Aktaş for their help in technical works.

Special thanks to Mine Bahçeci and Gökhan Erdoğan for their valuable suggestions and professional approaches during the characterization studies.

I also wish to thank Dr. Dan Perera for his comments on my differential scanning calorimetry analysis results.

Cafer Özgür prepared my sample holders voluntarily and he have taken great care.

Gözde Genç made very useful comments on scanning electron microscope analysis and she shared her industrial experiences with me, related to paint materials.

Ayben Top, Selda Göktaş and Şebnem Şimşek; my dear friends helped me sincerely whenever I met with a problem.

Thanks for Şerife Şahin Özalp for her patience in replying my numerous questions.

Finally my thanks are for my family, especially my parents Bilge and Latif Topçuoğlu and my brother Sedat Topçuoğlu for sharing my sleepless nights.

ABSTRACT

Sorption, diffusion and permeation data were obtained for water vapour in water borne acrylic paint films and in the pure binder of the paints which is methylmethacrylate-co-butylacrylate copolymer. Paint films which have the same formulation but contain different amount of binder were characterized to determine elements and their form, distribution of the ingredients, structure, functional groups, degradation temperature, glass transition temperature and roughness of the surfaces using energy dispersive X-ray (EDX), X-ray diffraction, map diagrams, scanning electron microscope, fourier transform infrared spectroscopy, thermal gravimetry, differential scanning calorimetry (DSC) and atomic force microscope, respectively.

Diffusivity and solubility of water in the paint films were measured at T= 30 ^{o}C while for the pure copolymer film similar data were collected at T= 30 ^{o}C and T= 40 ^{o}C, using a new type of gravimetric sorption apparatus called magnetic suspension balance. Fickian sorption is observed for both the paint films and the pure copolymer.

Diffusivity and permeability of water increases while the maximum water sorption capacity decreases with decreasing binder fraction in the paint films. Scanning electron microscope pictures and map diagrams show a nonhomogeneous distribution and flocculation of the pigments in the paint films with low binder content. Transport properties (diffusivity, permeability, water sorption capacity) of the pure copolymer are similar to those determined for the paint film containing 40% binder.

The sorption data for the paint films and the pure copolymer were interpreted using Flory-Huggins theory and ENSIC model, respectively. The Zimm and Lundberg cluster integral was used to determine the extend of clustering of water molecules. According to the predictions, water form clusters both in the paint films and in the pure copolymer. Degree of clustering and the change of mean cluster size with sorption appears to be larger for the pure copolymer.

ÖZ

Aynı formülasyona sahip fakat bağlayıcı madde oranları farklı su bazlı akrilik boya filmleri ile bu boya filmlerinin bağlayıcı maddesi olan metilmetakrilat-ko-bütilakrilat kopolimeri içerisinde su buharının sorpsiyon, yayınım ve geçirgenliğine dair veriler elde edilmiştir. Boya filmleri, yapılarında yer alan elementler ile bulundukları formların, dağılımlarının, genel olarak yapının, fonksiyonel grupların, bozunma ve camsı geçiş sıcaklıkları ile yüzey pürüzlülük değerlerinin bulunması amacıyla enerji dağılımı X ışınları (EDX), X ışınları kırınımı, harita diagramları, taramalı elektron mikroskopu, fourier transform kızılötesi spektroskopisi, termal gravimetri, taramalı diferansiyel kalorimetri ve atomik kuvvet mikroskopu kullanılarak karakterize edilmişlerdir.

Suyun boya filmleri içerisindeki yayınım ve çözünürlüğü ağırlık ölçümüne dayalı yeni tip bir sorpsiyon cihazı olan manyetik askılı terazi kullanılarak 30 ^{o}C sıcaklıkta ölçülürken benzer veriler saf kopolimer filmi için 30 ^{o}C ve 40 ^{o}C' de toplanmıştır.

Azalan bağlayıcı miktarına paralel olarak boya filmlerinin yapılarında barındırabilecekleri maksimum su tutma kapasitelerinde bir azalma görülürken suyun yayınım ve geçirgenlik katsayısı değerlerinde artış gözlenmiştir. Taramalı elektron mikroskop resimleri ve harita diagramları bağlayıcı içeriği az olan boya filmlerinde pigmentlerin homojen bir şekilde dağılmayarak topaklaşmalar oluşturduklarını göstermiştir. Saf kopolimerin taşınım özelliklerinin (yayınım, geçirgenlik, su tutma kapasitesi) %40 bağlayıcı içeren film için elde edilen değerlere yakın olduğu belirlenmiştir.

Boya filmlerinin ve saf kopolimerin sorpsiyon verisi sırasıyla Flory-Huggins teorisi ve ENSIC modeli kullanılarak değerlendirilmiştir. Zimm ve Lundberg'in geliştirdiği model kullanılarak su moleküllerinin filmler içerisinde ne derece kümelenme oluşturdukları belirlenmiştir. Hesaplamalara göre, su hem boya filmleri hemde saf kopolimer içerisinde kümelenmeler oluşturmaktadır. Kümelenmenin derecesi ve ortalama kümelenme büyüklük değerinin saf kopolimerde artış gösterdiği tespit edilmiştir.

TABLE OF CONTENTS

LIST OF FIGURES

LIST OF TABLES

NOMENCLATURE

A	:Area of the membrane; (cm^2)
a_w	:Activity of water vapour
C	: Concentration of penetrant molecules; (mol/cm^3)
C_{eq}	: Penetrant concentration at equilibrium; (mol/cm^3)
C_o	:Initial concentration of the penetrant in the film; (mol/cm^3)
C_{1L}	:Concentration of the permeant at lower surface of the membrane; (mol/cm^3)
C_{1u}	:Concentration of the permeant at upper surface of the membrane; (mol/cm^3)
D	:Diffusion coefficient; (cm^2/s)
D_{eff}	:Effective diffusion coefficient; (cm^2/s)
D_0	:Diffusion coefficient at initial concentration; (cm^2/s)
G_{ww}	:Cluster integral
J	:Mass flux; (g/cm^2s)
J_1^o	:Mass diffusion flux of solvent relative to velocity of polymer; (g/cm^2s)
k_p	:Polymer-penetrant interaction parameter for ENSIC model
k_s	:Mutual penetrant interaction parameter for ENSIC model
L	:Thickness of the film; (cm)
M_o	:Mass of the film at initial time; (gr)
M_t	:Mass of the film at any time; (gr)

M_∞ :Mass of the film at equilibrium; (gr)

P_{eff} :Effective permeability coefficient; (mol/cm^{3}skPa)

$P_{solvent}$:Solvent vapour pressure; (kPa)

P_{1L} :Partial pressure of the permeant in lower compartment; (kPa)

P_1^0 :Saturated vapour pressure of the solvent; (kPa)

P_{1u} :Partial pressure of the permeant in upper compartment; (kPa)

P_{1ui} :Partial pressure of the permeant in upper compartment at initial time; (kPa)

$P_{1u(t)}$:Partial pressure of the permeant in upper compartment at any time; (kPa)

q_1 :Concentration variable; (gr/ cm^3)

q_1^* :Dimensionless concentration variable of the solvent

q_{1E} :Equilibrium concentration variable of solvent; (gr/ cm^3)

q_{1o} :Initial concentration variable of the solvent; (gr/ cm^3)

q_{2o} :Initial concentration variable of the polymer; (gr/ cm^3)

R :Gas constant; (cm^{3}kPa/mol.K)

RH :Relative humidity; (%)

S_{eff} :Effective solubility coefficient; (mol/cm^{3}kPa)

T :Temperature; (K)

T_g :Glass transition temperature; (K)

T :Time; (s)

t^* :Dimensionless time

x :Coordinate in the direction of flux; (m)

v_1 :Mass average velocity of solvent; (cm/s)

v_2 :Mass average velocity of polymer; (cm/s)

V_u :Volume of the upper cell; (cm^3)

V_w :Partial molar volume of the water; (cm^3/mol)

V_1 :Specific volume of the solvent; (cm^3/gr)

V_2 :Specific volume of the polymer; (cm^3/gr)

$\omega_{average}$:Average weight fraction of the penetrant in the film

$\omega_{equilibrium}$:Weight fraction of the penetrant in the film at equilibriums

$\omega_{initial}$:Initial weight fraction of the penetrant in the film

ω_1 :Weight fraction of the solvent

ω_{lo} :Initial weight fraction of the solvent

ΔH :Heat of decomposition of the binder; (kJ/kg)

χ :Flory-Huggins interaction parameter.

ϕ_w :Volume fraction of water in the polymer.

ξ :Length variable; (cm)

ξ_L :Quantity defined as $\xi_L = \rho_{2o} V_2 L$; (cm)

ξ^* :Dimensionless length variable defined by Equation (2.16)

ρ_1 :Mass density of the solvent; (gr/ cm^3)

ρ_2 :Mass density of the polymer; (gr/ cm^3)

α :Exponential constant used in defining concentration dependence of diffusion coefficient

CHAPTER 1

INTRODUCTION

Paints are often used for their decorative and protective functions. An underlying substrate can be easily deteoriated by the presence of moisture in the substrate or at the surface of the substrate. Deteoriating effects of water can be direct or indirect. When exposed to water in liquid or vapor form, paint eventually swells and peeling is observed. In addition, water in the paint favors corrosion reactions and growth of organisms, consequently paint losses its protective and decorative properties. To know the barrier properties of the paint, its water transport properties must be known. Nowadays, solvent borne paints are being substitued by water borne paints due to pressure of the regulations which aimed at reducing the emission of volatile organic compounds (VOCs). Success in chosing the most appropriate formulation for the water borne paints coming into the market depends on predicting drying rate of water from the paint which requires to know transport properties of water in the paint.

Previous studies have shown that paint ingredients which can be grouped as binders, solvents, pigments, additives, fillers and extenders have strong influence on structure of the paint films, hence on the diffusion process (Paul, 1985; Bierwagen, 1987; Brown et al., 1997; Barbucci et al., 1998; Corfias et al., 1999; van der Wel and Adan, 1999; George and Thomas, 2000; Bin Liu et al., 2002; Landolt et al., 2002).

The main objectives of this study are to measure permeability, diffusivity, and solubility, of water in water borne acrylic based paint containing methylmethacrylate-co-butylacrylate copolymer as a binder, to characterize structure of the paint films and to determine the relationship between the structure and transport properties.

In this study, the effect of binder content on the transport properties of water was investigated. For this purpose, four types of paints which have the same formulation but differ in the binder amount as 40%, 30%, 20% and 10% were utilized.

To find the relationship between the transport properties and the structure, these paint films were characterized using scanning electron microscope (SEM), energy dispersive X-ray (EDX), fourier transform infrared spectroscopy (FTIR), thermal

gravimetric analysis (TGA), differential scanning calorimetry (DSC), X-ray diffraction (XRD) and atomic force microscope (AFM).

Transport properties of small molecules in the polymers are measured by classical techniques given by Crank and Park (1968) and also by new advanced electronic, magnetic or nuclear magnetic resonance techniques (Mamaliga et al., 2003). In this study, magnetic suspension balance which is one of the most reliable and sensitive apparatus among other gravimetric sorption techniques was used to determine transport properties of water in both the paint films and the pure copolymer film. Sorption data were fitted by the Flory-Huggins theory and ENSIC model to be able to predict maximum water sorption capacity of the films. Thermodynamic models were also utilized to predict the extend of clustering and mean cluster size of water molecules.

From practical point of view, industry uses permeability coefficient of water to directly determine barrier properties of the paint films. Based on this concern, permeability of water in the paint and the pure copolymer films was also measured.

The thesis consists of four sections. The equations describing the sorption, diffusion and permeation processes are presented in Chapter 2. Chapter 3 gives general information about the paint and discusses the effect of its ingredients on diffusion behaviour of paint–penetrant systems. Experimetal techniques used for characterizing the samples and for measuring permeability, diffusivity and solubilities are discussed in Chapter 4. Experimental data and model predictions are discussed in Chapter 5 and general conclusions and possible suggestions for future work are summarized at the end of the thesis.

CHAPTER 2

MODELING OF DIFFUSION, SORPTION AND PERMEATION PROCESSES

In this chapter, typical sorption kinetics are discussed and equations describing the permeation process and the sorption process for both constant diffusion coefficient and variable diffusion coefficient cases are given. Furthermore, thermodynamic theories for modeling equilibrium isotherms are discussed.

2.1 Basic Equations

The transport of a penetrant molecule through a polymer film depends on the solubility of that penetrant molecule within that polymeric membrane and diffusivity through that system. The transport of some vapours in rubbery polymers follows a Fickian behaviour if the penetrant molecule is small enough that the relaxation motion of the polymer chains occurs in a faster rate in comparison to rate of diffusion of small penetrant molecules. For one dimensional case, Fickian type diffusion can be described by the Fick's first and second law;

$$-D\frac{\partial C}{\partial x} = J \tag{2.1}$$

$$\frac{\partial C}{\partial t} = \frac{\partial}{\partial x}(D(C)\frac{\partial C}{\partial x}) \tag{2.2}$$

In Equations 2.1 and 2.2, J is the the amount of permeant passing through the unit area of the film in unit time, D is the diffusion coefficient, C is the concentration of penetrant molecules, x is the coordinate in the direction of flux, and t is the time.

2.2 Modeling of Sorption Process

2.2.1 Constant Diffusion Coefficient Case

During the sorption process the paint films with a thickness of L are placed into the multi-tray sample holders in which one side of the films is exposed to the water vapour and the other side of the films is based on the impermeable wall of the sample holder. Important assumptions utilized to model this process is that the diffusion of water vapour through the polymeric based paint films is one dimensional Fickian type diffusion. There is no chemical reaction between the water vapour and ingredients of the paint material. The paint films are subjected to pure deionized water vapour. Finally, the vapour pressure of the water is small enough that at the end of each absorption step, the change in the thickness of the sample can be ignored and diffusion coefficient is independent of the concentration. Under these assumptions, sorption process is described by Equation 2.3;

$$\frac{\partial C}{\partial t} = D\frac{\partial^2 C}{\partial x^2} \tag{2.3}$$

Initially, the concentration of the water, C_o, in the paint is the same everywhere;

$$t=0 \rightarrow C= C_0 \tag{2.4}$$

At times greater than zero, the concentration of the penetrant at the surface is constant and equal to its equilibrium concentration, C_{eq}.

$$t>0 \rightarrow x= L \;\; C=C_{eq} \tag{2.5}$$

and concentration gradient at the lower surface is zero since it is impermeable to penetrant.

$$t>0,\ x= 0, \quad \frac{\partial C}{\partial x} = 0 \tag{2.6}$$

Analytical solution of the equations given in Equations 2.3 through Equation 2.6 is given by Crank (1975).

$$C(x,t) = -\frac{2C_0}{\pi}\sum_{n=1}^{\infty}\frac{1}{n}((-1)^n - 1)\sin\left(\frac{n\pi}{L}\right)xe^{-\left(\frac{n\pi}{L}\right)^2 Dt} \tag{2.7}$$

If Equation 2.7 is integrated between the limits of x = 0 to x= L then dimensionless uptake is obtained as follows;

$$\frac{M'_t}{M'_\infty} = \frac{M_t - M_0}{M_\infty - M_0} = 1 - \frac{8}{\pi^2}\sum_{m=0}^{\infty}\frac{1}{(2m+1)^2}\exp\left\{-D(2m+1)^2\pi^2 t/L^2\right\} \tag{2.8}$$

Crank has shown that at short times as t goes to zero, Equation 2.8 can be simplified as shown below;

$$\frac{M'_t}{M'_\infty} = \frac{2}{\sqrt{\pi}}\left(\frac{Dt}{L^2}\right)^{1/2} \tag{2.9}$$

Equation 2.9 points out that for short time interval, mass change curve becomes linear and diffusion coefficient value can be easily obtained from the slope of the $\frac{M'_t}{M'_\infty}$ versus $\sqrt{t}$ graph.

2.2.2 Variable Diffusion Coefficient Case

Experimental sorption curves are not properly described by analytical solution given by Equation 2.9 when both diffusion coefficient and the thickness of the film change through a particular step. In this case model equations to determine diffusion coefficients need to be modified. Recently Alsoy and Duda (2002) have analyzed unsteady- state sorption of a vapour or liquid by a polymer to investigate the influence of the moving phase boundary associated with polymer swelling and diffusion- induced convection. According to their formulation, the species continuity equations for the solvent denoted by 1 and polymer denoted by 2.

$$\frac{\partial \rho_1}{\partial t} + \frac{\partial (\rho_1 v_1)}{\partial x} = 0 \tag{2.10}$$

$$\frac{\partial \rho_2}{\partial t} + \frac{\partial (\rho_2 v_2)}{\partial x} = 0 \tag{2.11}$$

are converted to the following equation;

$$\left(\frac{\partial q_1}{\partial t}\right)_\xi + \left(\frac{\partial J_1^o}{\partial \xi}\right)_t = 0 \tag{2.12}$$

after introducing a diffusive flux $J_1^o = \rho_1 (v_1 - v_2)$, a new concentration variable, $q_1 = \frac{\rho_1}{\rho_2 V_2}$, and a new length variable $\xi(x,t) = \int_0^x \rho_2 V_2 dx$. If diffusive flux is expressed in terms of new length and concentration variables,

$$J_1^o = D(\rho_2 V_2)^2 \tag{2.13}$$

and is substitued into Equation 2.12, then the sorption process is described by the following equation:

$$\left(\frac{\partial q_1}{\partial t}\right)_\xi = \frac{\partial}{\partial \xi}\left[D(\rho_2 V_2^2) \frac{\partial q_1}{\partial \xi} \right] \tag{2.14}$$

Equation 2.14 is a nonlinear equation which is subject to the following initial and boundary conditions:

$$\left(\frac{\partial q_1}{\partial \xi}\right)_{\xi=0} = 0, \quad q_1(\xi_L, t) = q_{1E}, \quad q_1(\xi, 0) = q_{1o}, \quad \xi_L = \rho_{2o} V_2 L \tag{2.15}$$

This formulation can be put into a dimensionless form utilizing the following dimensionless variables.

$$q_1^* = \frac{q_1 - q_{1o}}{q_{1E} - q_{1o}} \qquad \xi^* = \frac{\xi}{\xi_L}, \quad t^* = \frac{tD_o}{\xi_L^2} \tag{2.16}$$

$$\frac{\partial q_1^*}{\partial t^*} = \frac{\partial}{\partial \xi^*}\left[\frac{D(\rho_2 V_2)^2}{D_o}\frac{\partial q_1^*}{\partial \xi^*}\right] \tag{2.17}$$

$$\left(\frac{\partial q_1^*}{\partial t^*}\right)_{\xi^*=0} = 0 \qquad q_1^*(1, t^*) = 1 \qquad q_1^*(\xi^*, 0) = 0 \tag{2.18}$$

In systems involving polymers, concentration dependence of small molecule in the film is usually described by an exponential function. Based on this fact, following expression can be proposed:

$$D = D_o \exp[\alpha q_1^*] \tag{2.19}$$

where the exponent α is allowed to vary with concentration as follows:

$$\alpha = \alpha_1 \exp[\alpha_2 (w_1 - w_{1o})] \tag{2.20}$$

At very low sorption rates, α approaches to zero, thus, diffusion coefficient remains constant ($D=D_o$).

The solution of equations (2.17) through (2.20) gives concentration of solvent in the film (polymer) as a function of position and time. When integrated, theoretical uptake curve is generated. The diffusion coefficient is obtained by minimizing the difference between the experimental and theoretical uptake curves.

2.3 Typical Sorption Kinetics

When the penetrant molecules diffuse through the polymeric systems, polymers can show different responses to this process. According to this response, sorption kinetics can be categorized as Case I, Case II and Case III diffusion (Ghi et al., 2000). Case I diffusion is also named as Fickian diffusion. In this case the rate of diffusion is significantly slower than the rate of relaxation of the polymer chains. In the Fickian

sorption when the fractional mass versus square root of time graph is drawn, firstly a linear part appears. Then the curve reaches to a saturation level. If the sorption process is a Fickian one, the desorption and absorption curves should overlap (van der Wel and Adan, 1999). In Case II diffusion, the rate of penetrant diffusion is greater than the rate of relaxation of the polymer chains. Case III sorption is also known as anomalous diffusion and this is a general name because there is not only one type of anomalous diffusion. Some of them are two-stage sorption and the others are sigmoidal sorption. As the name suggests, in the two stage sorption the curve exhibits two parts as firstly fast Fickian absorption and secondly slow non-Fickian absorption. In Sigmoidal sorption, S shaped curve is seen. Figure 2.1 shows typical sorption curves mentioned here.

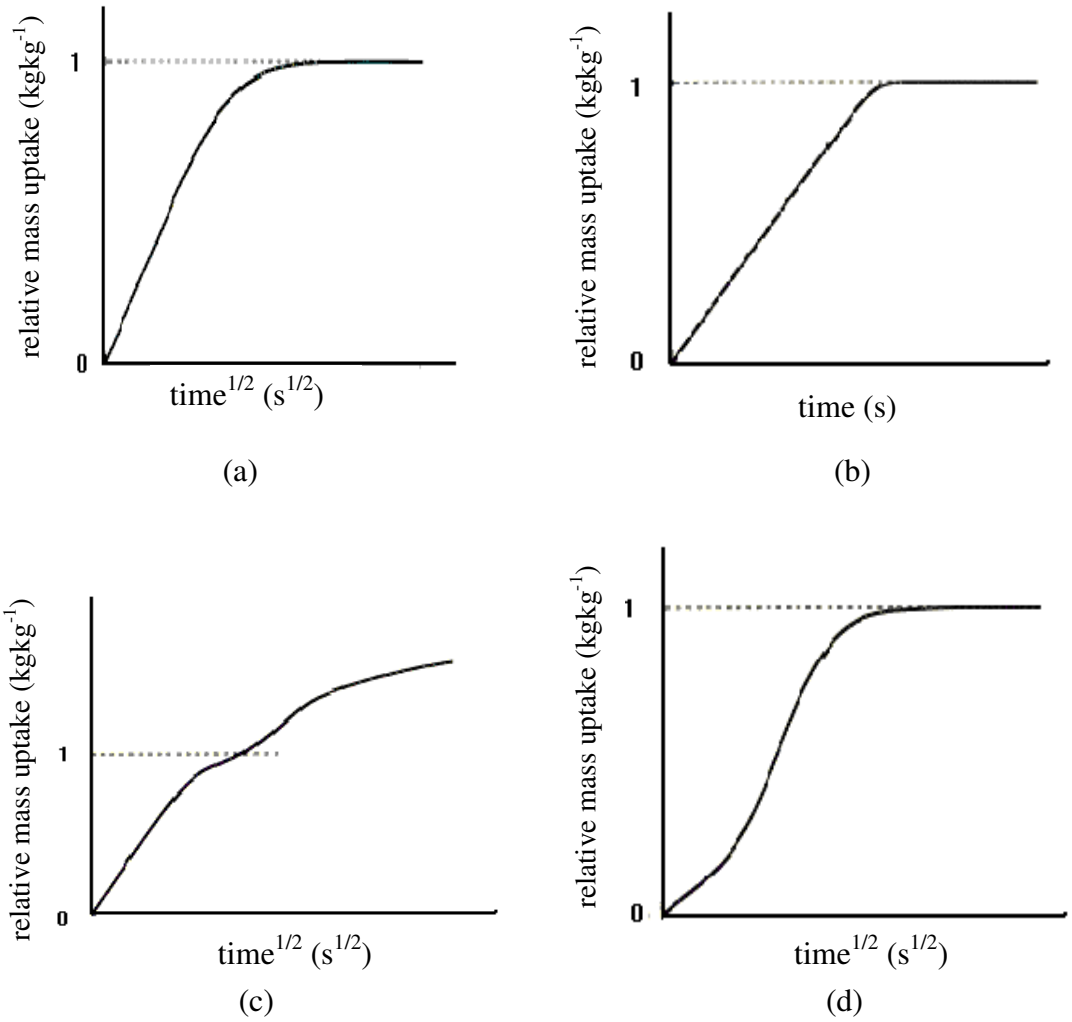

Figure 2.1: Typical sorption curves: a) Fickian absorption curve, b) Case II absorption curve, c) Two-stage absorption curve, d) Sigmoidal absorption curve (**Source**: van der Wel and Adan, 1999).

2.4 Modeling of Permeation Process

In the permeation experiments one side of the film with thickness L is exposed to the water vapour, which can be called as feed side and the other side is exposed to the atmosphere in the upper volume of the permeation cell and it can be called as permeate side. To model permeation process through paint films, it is assumed that transport through the films is one dimensional and can be represented by Fickian diffusion with an effective diffusivity, D_{eff}.

$$J = -D_{eff} \frac{\partial C}{\partial x} \tag{2.21}$$

Furthermore, it is assumed that film with a thickness of L is thin so that steady-state condition is achieved in the film even though the concentrations on the lower and upper compartments may change with time. If it is considered that diffusion coefficient is independent of concentration, then, Equation 2.21 can be integrated from x = 0 to x = L to find the following expression for the flux, J.

$$J = \frac{D_{eff}}{L}(C_{1L} - C_{1u}) \tag{2.22}$$

where C_{1L} and C_{1u} are the concentration of permeant at lower and upper surfaces of the membrane. If a linear equilibrium relationship between vapour and polymer phase exists,

$$C_{1L} = P_{1L}. S_{eff} \tag{2.23}$$

$$C_{1u} = P_{1u}. S_{eff} \tag{2.24}$$

then, amount of permeant passing through the membrane per unit time per unit area, J, is given as follows

$$J = \frac{D_{eff.}S_{eff}}{L}(P_{1L} - P_{1u}) \tag{2.25}$$

where P_{1L} and P_{1u} are partial pressure of the permeant in lower and upper compartments respectively. The product $D_{eff.}S_{eff}$ in Equation 2.25 is called as permeability coefficient, P_{eff}. Molecules permeating through the membrane cause an increase in partial pressure of the permeant in the upper volume of the cell. If vapour phase is assumed to be ideal, then an increase in pressure of the permeant is given by the following expression;

$$\frac{V_u}{RT}\frac{dP_{1u}}{dt} = J.A \tag{2.26}$$

where V_u is the volume of the upper cell, A is the area of the membrane and T is the temperature in the upper compartment. If Equations 2.25 and 2.26 are combined;

$$\frac{dP_{1u}}{dt} = \frac{RT}{L}\frac{A}{V_u}P_{eff}(P_{1L} - P_{1u}) \tag{2.27}$$

and if partial pressure of the permeant in the lower compartment is maintained constant, then Equation 2.27 can be integrated between the limits;

$$t = 0 \qquad P_{1u} = P_{1ui} \tag{2.28}$$

$$t = t \qquad P_{1u} = P_{1u(t)} \tag{2.29}$$

to give following expression;

$$\ln\frac{P_{1L} - P_{1ui}}{P_{1L} - P_{1u(t)}} = \frac{P_{eff}ART}{VL}t \tag{2.30}$$

Permeability coefficient, P_{eff}, can be calculated from the slope of $\ln\frac{P_{1L} - P_{1ui}}{P_{1L} - P_{1u(t)}}$ vs time graph.

2.5. Modeling of Equilibrium Isotherm

The Flory-Huggins thermodynamic theory is used for correlating the water sorption isotherms (Barrie, 1968; Perrin et al,. 1997; Rodriguez et al., 2003). Barrie (1968) notes that the theory is useful for describing water sorption behaviour in hydrophobic polymers. Perrin et al. (1997) showed that the water sorption isotherm in hydrophilic cellulose acetate can be well described by the Flory-Huggins theory for activities less than 0.7.

According to the Flory-Huggins theory, the relation between activity of water vapour, a_w, and its volume fraction in the polymer, ϕ_w is given as follows (Prausnitz et al., 1986).

$$\ln a_w = \ln\varphi_w + (1-\varphi_w) + \chi(1-\varphi_w)^2 \tag{2.31}$$

In this expression, χ represents the Flory-Huggins interaction parameter which provides how much a penetrant can dissolve the polymer. If χ value is less than 0.5, then the penetrant is a good solvent for the polymer.

The deviation from the Flory-Huggins thermodynamic theory especially at high penetrant activities lead to another approach derived by Perrin (Perrin et al., 1997). This model called as ENSIC model takes into account both penetrant-polymer and penetrant-penetrant interactions by introducing a second interaction parameter, k_s for mutual penetrant interactions. The interactions between the polymer and penetrant are reflected by the parameter k_p, which is comparable to the Flory-Huggins interaction parameter χ. These two constants are related to the penetrant volume fraction in the polymer by the following equation.

$$\varphi_w = \frac{\exp\left[\left(k_s - k_p\right)a_w\right] - 1}{\left(k_s - k_p\right)/k_p} \tag{2.32}$$

The thermodynamic theories can also be used to determine extend of clustering. Water is a unique penetrant due to its polar nature, thus, it can hydrogen bond with itself

and can form clusters. Zimm and Lundberg describe a mathematical approach to determine the extend of clustering based on a cluster integral, G_{ww}, which can be calculated from the equilibrium sorption isotherm as follows (Rodriguez et al., 2003)

$$\frac{G_{ww}}{V_w} = -(1-\varphi_w)\left[\frac{\partial(a_w/\varphi_w)}{\partial a_w}\right]_{P,T} - 1 \qquad (2.33)$$

where V_w is the partial molar volume of the water. The quantity G_{ww}/V_w indicates whether clustering takes place or not. If $G_{ww}/V_w = -1$, the solution is ideal, indicating that water molecules do not affect the distribution of other water molecules. If $G_{ww}/V_w>0$, water molecules tend to cluster, whereas if $G_{ww}/V_w<-1$, the water molecules prefer to remain isolated.

CHAPTER 3

GENERAL INFORMATION ABOUT PAINT AND EFFECTS OF ITS INGREDIENTS ON DIFFUSION BEHAVIOUR OF PAINT-PENETRANT SYSTEMS

In order to protect the surfaces from some corrosive, deteoriating materials and obtain aesthetic appearance, one of the most effective and commonly used way is to coat the surfaces with paints. Paint has a complex structure containing many functional ingredients. The properties of paint such as adhesion, color, thickness, viscosity, drying time and barrier property are strongly influenced by its ingredients.

In the first part of this chapter, general information about the paint ingredients are given. In the second part, the effects of paint ingredients on diffusion process are discussed.

3.1 Ingredients of Paint Material

Generally paint constituents are grouped in five categories: vehicles, solvents, pigments, additives, fillers and extenders (Weismantel, 1981; van der Wel and Adan, 1999). Polymer also named as vehicle is the binder material in which other ingredients are solubilised or dispersed. They represent the matrix structure of the coating and they are key elements to predict the durability of the coating (Bierwagen, 1987). Solvents adjust the viscosity of the paint material, pigments give the desired color to the paint while additives increase the stability of the paint material.

3.1.1 Vehicles

The vehicle is responsible from a continious paint film formation and well adhesion to the substrate. The vehicles are divided into six groups as solid thermoplastic film formers, lacquer- type film formers, oxidizing film formers, room temperature

catalyzed film formers, heat cured film formers and emulsion type film formers (Weismantel, 1981).

3.1.2 Solvents

Solvents are used to improve the application properties of paint materials. Most important function of a solvent is to reduce viscosity sufficiently so that the coating can be easily applied. In addition, solvents control levelling, flow, gloss, drying time and durability. Solvents dissolve the film former of coating solution. They separate and keep apart the droplets of film former in emulsion coatings.

Paints are categorised as waterborne and solvent borne paints. For the solvent borne paints, solvents are often classified as hydrocarbons and oxygenated solvents. Hydrocarbon solvents are grouped as aliphatic and aromatic. They differ in the way in which the carbon atoms are connected in the molecule. This characteristic structural difference affects the chemical and toxicological properties of the solvent (Weismantel, 1981).

In water borne paints, function of solvent is performed by water. Water borne coatings have low viscosity so brushability is higher and their flammability is lower. In addition, they are environmentally friendly products, since the emission of volatile organic compounds from solvent borne coatings is a major concern. However, the disadvantages of water borne coatings may arise from their easy foaming properties and high cost. Furthermore, drying time for water borne paints is longer and some defects in the form of cracks are frequently observed and water may react with some materials (Kristoffersson et al., 1998). The most common applications of water borne coatings is latexes. Latex can be defined as a stable colloidal dispersion of a polymeric substance in an aqueous medium. Microstructure development of latex coatings can be divided into three stages: 1)Water evaporation and transformation from a suspension to a porous medium. 2) Deformation of latex particles due to capillary pressure 3) Final coating properties development (gloss, opacity, brightness) formed by heat, pressure, aging etc. (Keddie, 1997; Kristoffersson et al., 1998; Le Pen et al., 2003). In comparison to water soluble polymers (water can dissolve the binder) polymeric content of the latex is higher and at the same time viscosity does not increase, due to the low glass transition temperature, there is no need to add plasticizer (Kristoffersson et al., 1998).

3.1.3 Pigments

Paint pigments are solid grains or uniform size particles (Weismantel, 1981). They are insoluble and dense substances which are suspended into the coating formulation (van der Wel and Adan, 1999). Paint pigments must be unreactive to perform their functions. According to their origin and compositions, pigments are classified into three groups as inorganic, organic, and dispersed pigments (Paul, 1985).

Three important aspects of pigmentation are opacity, color and gloss control. Opacity is the ability of paint to hide the substrate. Color is due to the ability of pigments to absorb certain wavelenghts of visible light and reflect the other wavelenghts. Pigments also control the gloss of paint by affecting the texture of the coating surface (Weismantel, 1981). By absorbing UV radiation pigments prevent the degradation of the polymer. Pigment absorbtion spectra and whether the pigment has photocatalyst property or not are important subjects for a good protection. Some of the most popular pigments are titanium dioxide, iron oxide, aluminium flakes and zinc oxide.

3.1.4 Additives

Additives are used in relatively small amount to improve the performance of coatings (Weismantel, 1981; van der Wel and Adan, 1999). Some necessary properties which cannot be supplied by the binder or pigments are given by additives to the paint. Additives also improve certain properties of the vehicle like speed of drying, and resistance to fading (Weismantel, 1981). The most important additives are pigment dispersants, rheology modifiers, levelling additives, and antifoams. Antifoams prevent foam formation. Levelling agents facilitate spreading of the paint over the substrate surface and homogeneous film formation. Rheology modifiers are used to adjust the viscosity of paint. Pigment dispersants supply well, homogeneous distribution of the pigments through the paint (van der Wel and Adan, 1999).

3.1.5 Fillers and Extenders

Fillers are generally used to lower the paint price. They increase the hardness of the paint material. Talc, clay, chalk, quartz, are the filler materials used for these purposes (van der Wel and Adan, 1999).

Extenders are type of inorganic pigments. They are mainly added to the paint systems to a) control the rheological properties of paints, b) reduce settling tendency of pigments, c) improve flow properties, d) reduce gloss, e) increase the opacity of white hiding pigments, f) improve mechanical properties, g) increase the barrier properties of paint films (resistance of films towards diffusion of water and agressive gases) (Paul, 1985).

3.2 Effects of Paint Ingredients on Diffusion Process

Transport properties of polymers may exhibit differences when they are used as paint constituents. Because, besides polymer; paint consists of pigments, solvents, additives, fillers and extenders, and each of these ingredients affects transport behaviour (van der Wel and Adan, 1999).

3.2.1 Effects of Pigments on Diffusion Process

To obtain a high quality paint essential amount of pigments must be contained in the paint material due to their useful contributions. The amount of pigments and fillers relative to the amount of binder is known as pigment volume concentration (PVC). It is known that inorganic pigments and extenders are dense, and impermeable substances and their solubilities are less or they are non soluble. Because of these properties, pigments improve the barrier properties of paints. In order to perform their functions all of the pigments must be completely wetted by the binder material. Thus, binder should be found in the paint in a sufficient amount. When the amount of binder is such that the total pigment volume is completely wetted, PVC is called as critical pigment volume concentration (CPVC). If the amount of pigments is increased unlimitedly, percentage of binder decreases to a very low amount, in other words if CPVC is exceeded all of the pigments cannot be wetted by the binder material

completely. In this case, the structure of the paint becomes porous and the rate of water transport through the paint increases. Consequently, the barrier properties of the paint significantly decreases. Bin Liu et al., (2002) investigated the effect of changing pigment amount on the water vapour diffusion behaviour of alkyd based coatings. They used micaceous iron oxide as the pigment material in the coatings and PVC was changed as 40%, 50%, 60%, and 70%. Their results have shown that diffusion coefficient of water in the coating decreased when PVC increased up to 60% as illustrated in Figure 3.1. Based on these results, they have concluded that 60% corresponds to CPVC above which pigment binder interface becomes porous due to insufficient wetting of pigments, thus, diffusion coefficient increases.

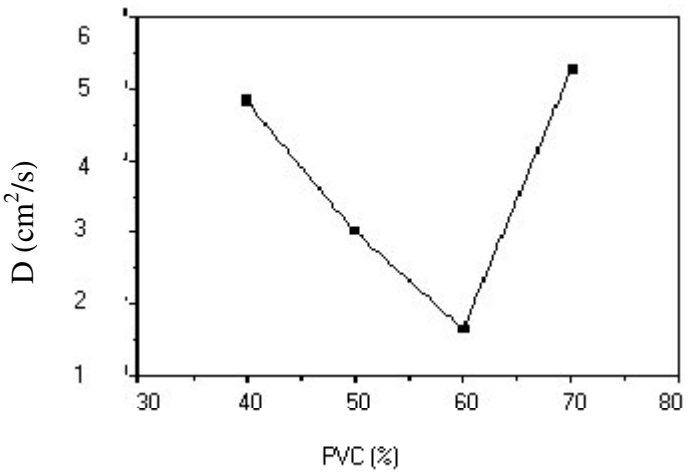

Figure 3.1: Effect of PVC on the diffusion coefficients of water diffusing through alkyd coatings (**Source:** Bin Liu et al., 2002).

Barbucci et al. (1998) also found that diffusion coefficient of water in flourinated coating changes with PVC. Their results are tabulated in Table 3.1.

Table 3.1: Diffusion coefficient of water in flourinated coatings at different PVC. (**Source**: Barbucci et al., 1999).

PVC	D (cm^2/s)
0	$2.5x10^{-5}$
7	$4.0x10^{-5}$
10	$2.1x10^{-5}$

Not only the binder amount but also the size, shape and the geometry of the pigment influence the CPVC (Paul, 1985) and coating durability (Bierwagen, 1987). In an ideal case of pigmentation, the pigments should be well dispersed. Degree of dispersion of the pigment is closely related to the coating protection capacity since pigments and polymer interact in the coating. Moreover, if flocculation occurs, the pigment particles cannot be wetted completely and the wetting process is not successful. For this reason even if the CPVC is not exceeded, due to the insufficient wetting of the pigments, a porous structure can be observed and barrier property of the paint decreases. Brown et al. (1997) studied the effect of PVC and the size of the latex particles on the pigment distribution in water-borne coatings. They reported that heterogeneous distribution and forming clusters in the pigment crystals cause to high water vapour permeability in emulsion paints. They stated that pigment clustering is due to size and size distribution of latex particles as well as the number and size distribution of the pigment particles.

3.2.2 Effects of Additives and Fillers on Diffusion Process

Paint is a very complex structure containing many groups. The polarity of these groups are usually different from each others, especially in water borne paints, the polarity difference between the groups increases. One of the important functions of the additives is to enable compatibility between these different groups in the paint. However, additives are known as hydrophilic materials, thus, they cause an increase in water permeation rate and a decrease in barrier property of the paint (van der Wel and Adan, 1999). One of the commonly used additives are pigment dispersants. They provide a physical barrier around pigment particles to prevent flocculation (Brisson and Haber, 1991). In order to investigate the type of dispersion agent on the barrier properties of water borne epoxy coating, Landolt et al. (2002) performed experiments by using two types of coating with the same formulation containing polyacrylic acid and polyamine salt as dispersing agent. In Figure 3.2 water uptake behaviours of the coatings were represented. According to the figure, water uptake values of the coating which contain polyacrylic acid is higher which means that it has relatively bad barrier properties in comparison to the coating containing polyamine salt. This result showed

that the type of dispersing agent used in the paint significantly affects the barrier properties of the coating.

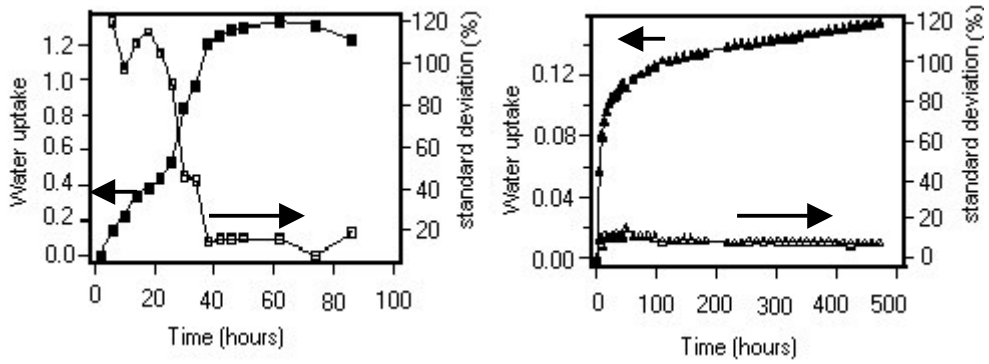

Figure 3.2: Water uptake as a function of immersion time: (a) for the coating containing polyacrylic acid and (b) for the coating containing polyamine salt (**Source:** Landolt et al., 2002).

The diffusion process in the polymeric systems also depends on the type of the filler. If the filler added to the polymer is compatible with the polymer matrix, it is expected to cause decreasing free volume within the polymer matrix and forming a torturous path for the permeating molecules. Geometrical properties of the filler material influence the tortuosity. In the case of incompatible filler usage, pores form at the filler-polymer interface so permeability increases (George and Thomas, 2000). Corfias et al. (1999) investigated the effect of fillers on the barrier properties of polyurethane based film coated on galvanized steel. In the experiments three types of coating with different filler materials were used, for all of the coating materials the binder material was polyurethane. A clear coat (binder alone), coating with alumina silicates, coating with neutral fillers and chromates were used in the experiments. Their results indicated that number of pores in the chromated system was low since chromates stabilized the structure of the coating due to electrostatic interactions. Thus, coating with chromate as a filler material was found to have better barrier property to water diffusion compared to other coatings.

CHAPTER 4

EXPERIMENTAL STUDIES

Experimental studies can be grouped into three categories as characterization, permeation and diffusion studies. In the first part of this chapter, all characterization techniques used to identify the structure of the paint films are introduced. In the second part, details of the experimental set-ups and procedures followed for measuring permeability and diffusivities are discussed.

4.1 Materials

In this study four types of paints which have the same formulation but differ in the binder amount as 40%, 30%, 20%, 10% were utilized. The binder used in paint formulation is methylmethacrylate-co-butylacrylate copolymer. Paint samples were supplied by Akril Kimya A.Ş. Some experiments were done by using binder alone (methylmethacrylate-co-butylacrylate copolymer) in order to compare the results obtained from the experiments in which paint samples were used. Binder material was supplied by Organik Kimya A.Ş in the form of an emulsion consisting of 50% copolymer, 50% water and 110 ppm residual methylmethacrylate.

4.2 Film Preparation Method

Paint films were prepared by casting the solution onto a clean and smooth glass substrate through an automatic film applicator (Sheen-1133N). For characterization studies, all paint films were prepared by using a blade with a thickness of 300 μm. For permeability and diffusion studies paint films were prepared using the blades with a gap of 120, 250, and 300 μm. In order to evaporate the water contained in the films, they were dried in the vacuum oven at 100 ^{o}C for an hour. Dried films were placed in a deionised water bath to detach them from the glass substrate easily. Duration time in the water bath was different for each film ranging from 30 seconds to 37 minutes. For the

final drying process the detached films were again replaced in a vacuum oven at a temperature of 100 ^{o}C for 72 hours.

4.3 Characterization Studies

4.3.1 Scanning Electron Microscope (SEM)

Scanning Electron Microscope (Philips XL 30 S FEG) was used to determine structure of the paint films from their opaque and glossy surfaces at various magnifications using secondary electron imaging (SEI) and back scattering (BS) detectors. In addition, cross sectional micrographs were taken to measure average thickness of the paint films using only SEI detector. At the same time SEI mode allowed to observe possible structural differences between opaque and glossy sides of the paint films. In BS mode, compositional contrast was seen in the images of the paint films, and this contrast was used to evaluate the distribution of different phases and compounds in the paint films.

4.3.2 Energy Dispersive X-ray (EDX)

EDX analysis was carried out on the opaque surfaces to determine the elements in the paint films. In this analysis, data were collected from 20 randomly chosen points and by taking arithmetic mean of these values, average weight percent of the elements found in the films was calculated.

The elements investigated in the EDX were represented by a different colour and map diagrams were formed. By using these diagrams, the degree of homogenity in the distribution of the elements in the paint films with different binder amount was observed.

4.3.3 Fourier Transform Infrared Spectroscopy (FTIR)

FTIR spectrophotometer (Shimadzu 8601 PC) was used to obtain functional groups in the paint samples. The resolution was 4 cm^{-1}. The range of the wavenumber was between 400 and 4600 cm^{-1}. Sensitive pyroelectric type of DLATGS (deuterium

triglyceride sulfide which is adapted by L-alanine) element was mounted on the FTIR – 8601 PC as a detector.

4.3.4 Thermal Gravimetry (TGA)

In order to observe changes in thermal events in the paint films related to changing binder amount, thermal gravimetric analysis was done by using Shimadzu TGA-51. The samples were placed into the alumina crucible. Weight of the samples was 8.683, 9.164, 7.989, 9.968 mg for the paint films which have 40%, 30%, 20%, 10% binder, respectively. Samples were heated up to 1000 ^{o}C with a heating rate of 10 ^{o}C/min. During the heating of the samples, nitrogen gas was used as the purge gas with a flow rate of 30 ml/min except that in the paint with 30% binder, the flow rate of the nitrogen gas was 40 ml/min. TG analysis of the pure copolymer with a weight of 9.46 mg was done under the same conditions except that the heating process was applied up to 600 ^{o}C.

4.3.5 Differential Scanning Calorimetry (DSC)

Differential Scanning Calorimetry (Shimadzu DSC-50) was used to determine the glass transition temperatures of the paint films. Films whose weights change between 2.6 –3.4 mg were placed into the aluminium crucible. Then, they were heated up to 500 ^{o}C with a heating rate of 1 ^{o}C /min until 30 ^{o}C and 5 ^{o}C/min above 30 ^{o}C using nitrogen as a purge gas with a flowrate of 40 ml/min.

4.3.6 X-Ray Diffraction (XRD)

Philips X'Pert Pro diffractometer was used to investigate the crystalline form of the elements present in the paint films. The operating conditions were 45 kV and 45 mA. CuKα radiation, λ = 0.15406 A^{o}, was carried out. The range for the X-ray scan was made over 2θ values of 5-70 ^{o}C with a scan speed of 0.06^{o}/second. X'Pert Graphics & Identify software was used to record the XRD intensities. The data collector was X'Pert data collector. The crystalline peaks were identified by matching

with standard reference patterns from PCDFWin database maintained by the International Centre for Diffraction Data (ICDD).

4.3.7 Atomic Force Microscope (AFM)

AFM was used to measure the roughness of the paint films. Analysis was done by using Digital Instrument Multimode Nanoscope SPM 4, and both in contact mode. The measurements were carried out in ambient air. In contact mode, OTR8-35 Si cantilever was used. The lenght of the cantilever and the resonance frequency were between 100-200 μm and 73-24 kHz, respectively.

4.4 Solid-Liquid Ratio Analysis

The solid-liquid ratio of the liquid paint samples and also pure copolymer were investigated by using Sartorius Moisture Analyzer (MA 100) device. The liquid samples were cast onto the aluminium pans and the initial mass of the samples and the tares of the pans were measured in the Sartorius Electronic Balance that has a resolution of 0.1 mg. Standard drying was selected as heating program and the temperature was set to 70 ^{o}C. Until the temperature reach the set value, an empty pan was placed into the device. While changing the pans, the maximum temperature deviations caused by opening of the device is 4 ^{o}C for a minute. Thus, it could be said that the drying kinetics of the samples was studied under constant temperature. Drying period in the moisture analyzer device was two hours. At the end of the first drying period, the dried samples except pure copolymer were placed into a vacuum oven which works under vacuum at 80 ^{o}C. At certain time intervals, weight of the samples was measured and the drying process continued until no change in weight of the samples was observed which lasted for two weeks.

4.5 Permeability Studies

Permeability studie were performed in a vessel consisting of three separable parts as shown in Figure 4.1. A schematic diagram of the permeability set up is illustrated in Figure 4.2. The bottom part contains a small bath filled with the solvent

used in the permeability studies. In this study, deionized water, 2.9% and 5% (by weight) NaCl solutions were used as solutes. The middle part of the set up consists of a hole whose diameter is 3.83 cm. The inside diameter of the middle part is 5.8 cm. Films were cut in such a manner that their diameters are nearly equal to the inside diameter of the middle part so that area of the hole is fully covered. The films were placed into the section by using vacuum gress oil. The ring was put over the films to keep the constant position of the films and prevent any possible leakage which may be seen in the areas other than effective hole area. In most of the experiments the rings were renewed in order to prevent contamination which may remain from the previous experiments. The last part which is the upper part of the permeation set up consists of a probe to read the humidity of the upper section. When the solvent transport proceeds through the films, an increase in relative humidity of the upper section is read by the probe and the relative humidity, time and temperature data collected are stored in the internal memory of the probe (Datalogger SK-L 200 TH).

During typical permeation experiments the bottom of the middle part was covered tightly with the parafilm and then the film under investigation was placed to the upper part of the middle section and ring was placed over the film. The upper part which contains humidity sensor was linked to the middle section and exposed to dry air during six hours. Just before the drying air was passed through the system, the initial humidity was recorded. These humidity values changed from one experiment to another between the range of 29.9- 58.3%. Drying of the films was performed by using an air pump (EP-6500). First of all, the air was pumped to the drying column which contains anhydrous $CaSO_4$ and molecular sieve 5A and then it was transported to the upper part of the permeation set up with a flowrate of 610 ml/min. At the end of the drying process, the humidity of the upper section was completely lowered to the value of 5%. The purpose of drying the upper part of the films was to remove water in the films. As it was explained in the film preparation method section, the films detached from the glass substrate were placed into the oven which works under vacuum at 100 ^{o}C during 72 hours. However, when they are exposed to the atmosphere, they absorb some amount of water vapour from the air due to the concentration gradient. Another reason for six hours drying was to allow uniform concentration in the upper part of the set-up. After the drying process was completed, the parafilms under the middle section was removed and the middle and upper sections was linked together to the bottom section. The set up was completely tighted by the help of steel rings placed on top of the upper part and

when tight connection was provided between all parts of the device, computer program was immediately started to record increasing relative humidity values caused by the water transport through the membrane. Time interval to collect the relative humidity and temperature data was selected as 10 seconds.

Figure 4.1: Digital photograph of the permeation set-up.

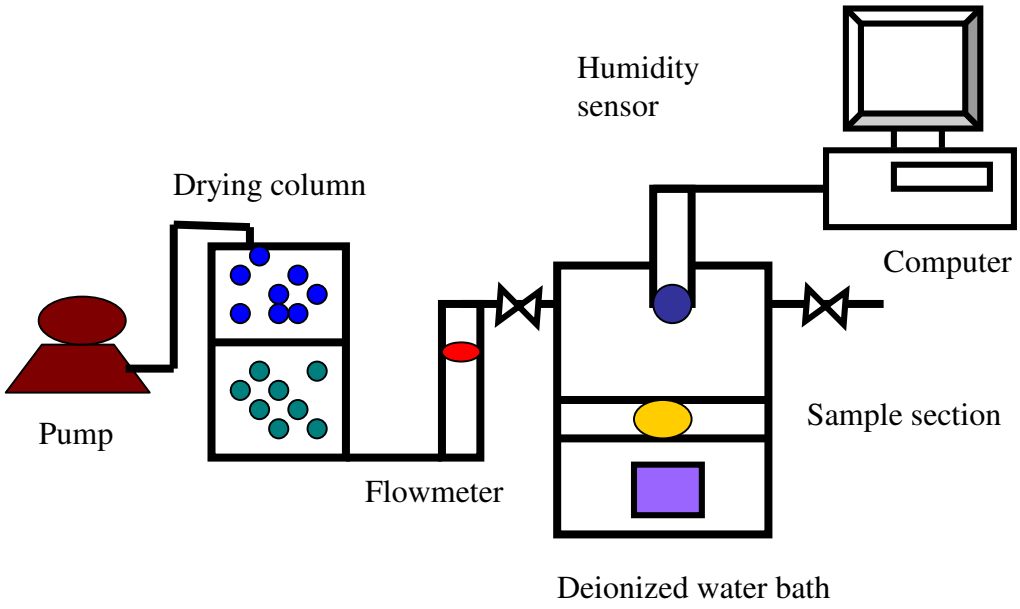

Figure 4.2: Schematic diagram of the permeation set-up

4.6 Diffusion Studies

4.6.1 Magnetic Suspension Balance

Magnetic Suspension Balance consists of four groups as main sorption column, controlling unit, computer and supporting units as shown in Figure 4.3. Main sorption column consists of microbalance, suspension magnet, coupling housing, measuring load decoupling, thermostats and the measuring cell. Electromagnet is inside the microbalance. The resolution of the microbalance is 1 μg, the maximum load is 5 g, and the reproducibility of the measurements is ± 2 μg. The operating pressure and temperature of the column are 150 bars and 250 ^{o}C, respectively. The important parts of the supporting units are water bath, vacuum pump, pressure gauge, solvent flask, and cold trap. The function of the water bath (accuracy is ± 0.5 ^{o}C, and the operating range is between 5 and 150 ^{o}C) which stands near to the column is to keep the main sorption column at a desired temperature. The vapour pressure of the solvent is measured by a pressure transducer operating within the range of vacuum up to 1 atm. with an accuracy of 0.25 % full scale. Vacuum is applied to the column by using rotary vane pump which can apply vacuum up to 0.0001 mbar. A cold trap is installed between the sorption column and the vacuum pump in order to prevent the corrosion of vacuum pump caused by the suction of the solvent vapours in the column. Solvent vapour is prepared in a solvent flask inserted into a constant temperature bath.

In diffusion experiments, multi-tray sample holder was used to place the films into the measuring cell. Before experiments are started, the column was heated up to 60 ^{o}C by using water bath and during the heating of the column, vacuum was applied in order to remove water desorbed by the paint films due to this heating process. Then, the program in the software was started and the system is allowed to reach equilibrium in 24 hours. After this preliminary part was completed, experiments were performed in two ways. In one way, sorption process was started by sending the solvent vapour at room temperature to the system. For this purpose, solvent vapour was trapped in the line between the column and solvent valves. The pressure gauge reads the saturated pressure of the solvent at the ambient temperature. Meanwhile the program in the software was started and the weight differences under vacuum was recorded until 4-30 measuring data points were supplied. Then the column valve was opened and solvent vapour was

sent into the column. This procedure was repeated until the operating pressure of the solvent vapour becomes equal to the saturated vapour pressure of the solvent in the flask at that temperature. In the second way, vapour-liquid equilibrium at a desired temperature was attained in the solvent flask and solvent vapour was sent to the column by opening the valves. After the polymer sample reached to the equilibrium state, the valve was closed and a sudden change in the vapour pressure of the solvent was induced by increasing the temperature of the constant temperature bath. Then, solvent vapour at a new vapour pressure level was sent to the column. This procedure was repeated until temperature of the solvent vapour in the flask reached to 5 ^{o}C below the temperature of the column.

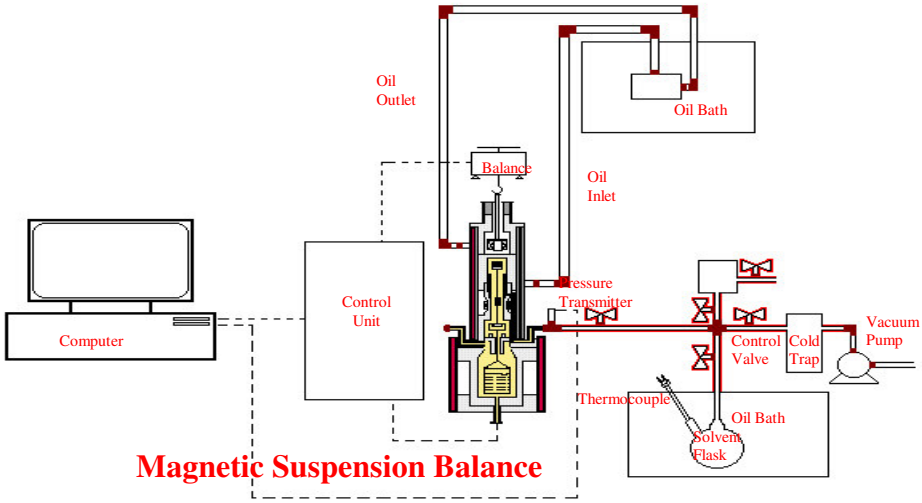

Figure 4.3: Schematic diagram of experimental set-up for measuring sorption and diffusivities.

CHAPTER 5

RESULTS AND DISCUSSIONS

In this chapter, first of all the results of characterization studies are discussed. Then, permeability and equilibrium sorption studies are discussed. Finally, the results of diffusion studies are given.

5.1 Characterization of the Paint Films

5.1.1 Determination of the Thickness and Morphology of the Paint Films Using Scanning Electron Microscope

Figures 5.1 through 5.4 show the scanning electron micrograph pictures of the paint films having 40%, 30%, 20%, 10% binder, respectively. Thickness of each film listed in Table 5.1, was determined from an average of 6 or 7 measurements.

Table 5.1: Average thickness of the paint films.

Sample	Number of points taken for thickness measurements	Average thickness (micron)
40% Binder	6	106.7
30% Binder	7	100.2
20% Binder	6	116.6
10% Binder	6	141.3

From the figures it can be seen that the structure of the paint films having 40% and 30% binder exhibits similarities with each other. These paint films have relatively less porous structure in comparison to paint films having 20% and 10% binder. The structural similarity also exists for the paint films having 20% and 10% binder. According to the cross sectional micrographs, the porosity of these films is relatively high.

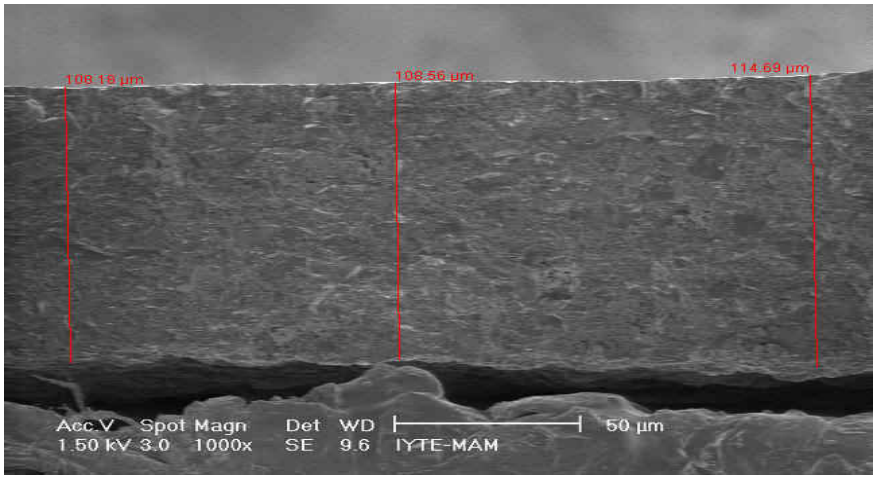

Figure 5.1: Scanning electron micrograph taken over the cross section of the paint. Binder content: 40%

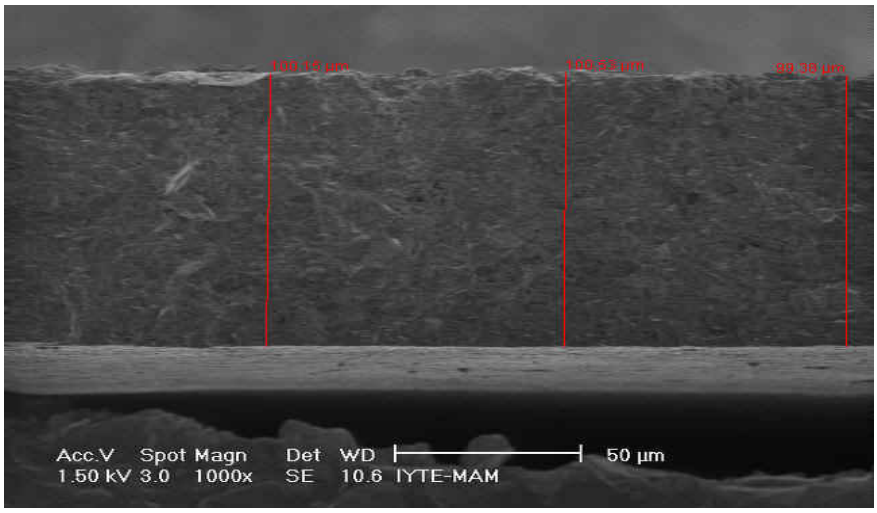

Figure 5.2: Scanning electron micrograph taken over the cross section of the paint. Binder content: 30%

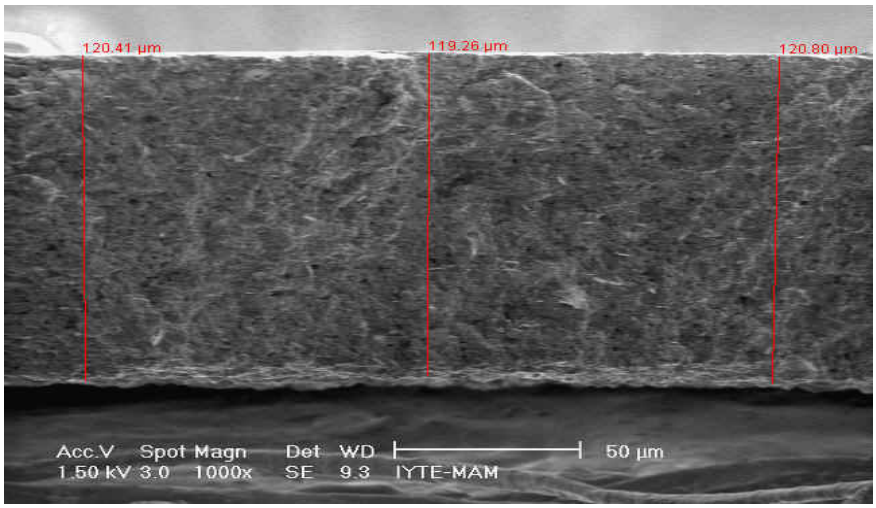

Figure 5.3: Scanning electron micrograph taken over the cross section of the paint. Binder content: 20%

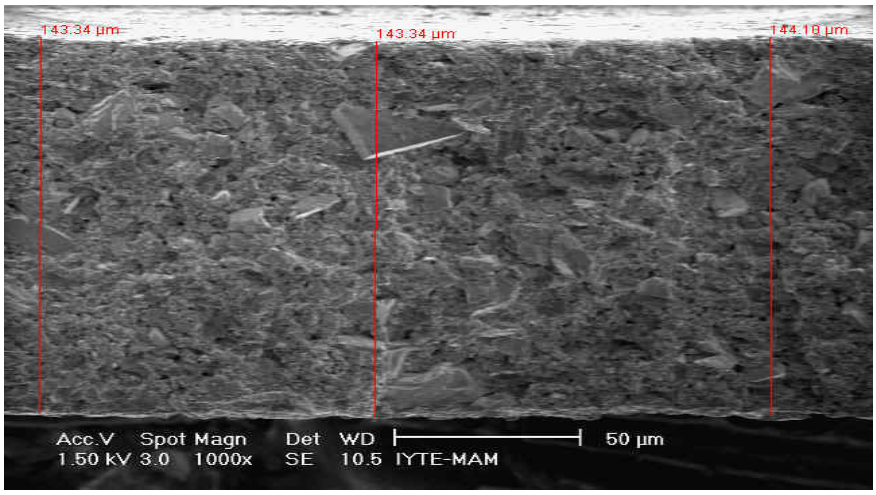

Figure 5.4: Scanning electron micrograph taken over the cross section of the paint. Binder content: 10%

5.1.2 Surface Micrographs of the Paint Films

When the paint films are detached from the glass substrate, it was observed that, the side which is back to the substrate is smooth and glossy, while the side which is exposed to the air is rough. For this reason, micrographs were taken from both sides of the films to observe any possible difference in the surface structure of the paint films as shown in Figures 5.5 through 5.8.

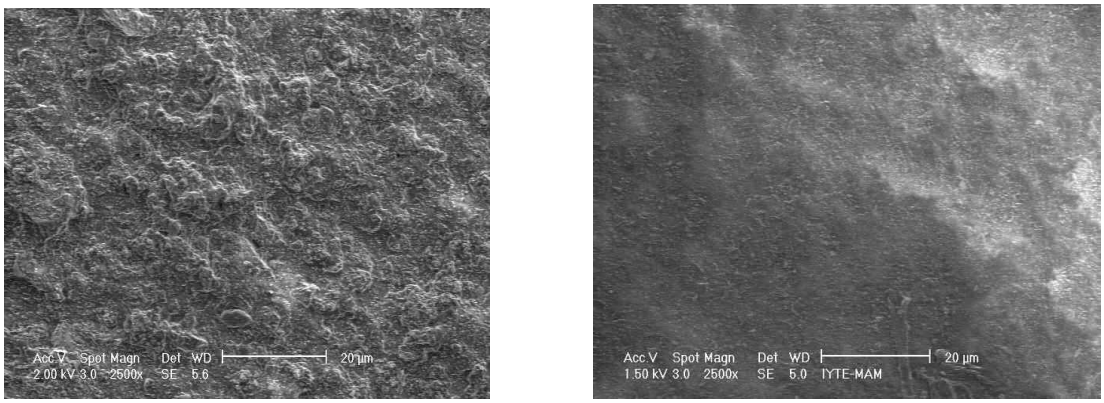

(a) (b)

Figure 5.5: Surface micrographs of the paint having 40% binder at 2500 magnification; (a): opaque side, (b): glossy side.

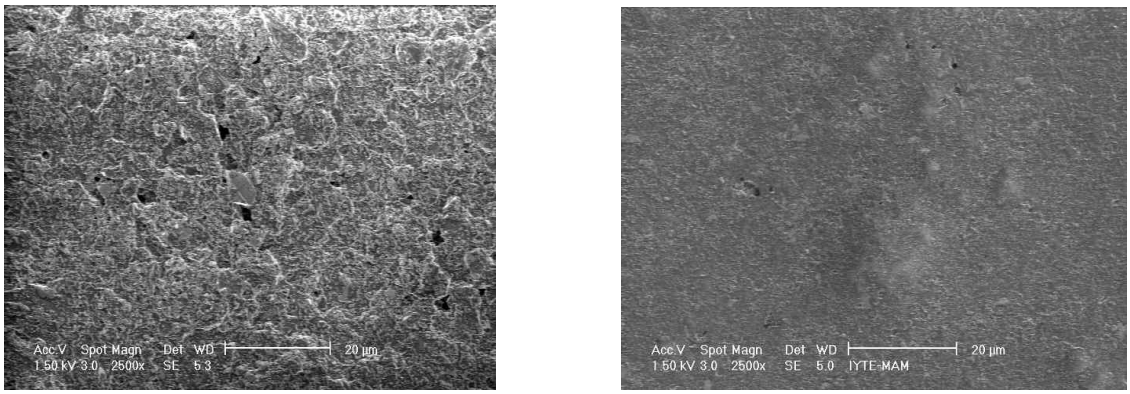

(a) (b)

Figure 5.6: Surface micrographs of the paint having 30% binder at 2500 magnification; (a): opaque side, (b): glossy side.

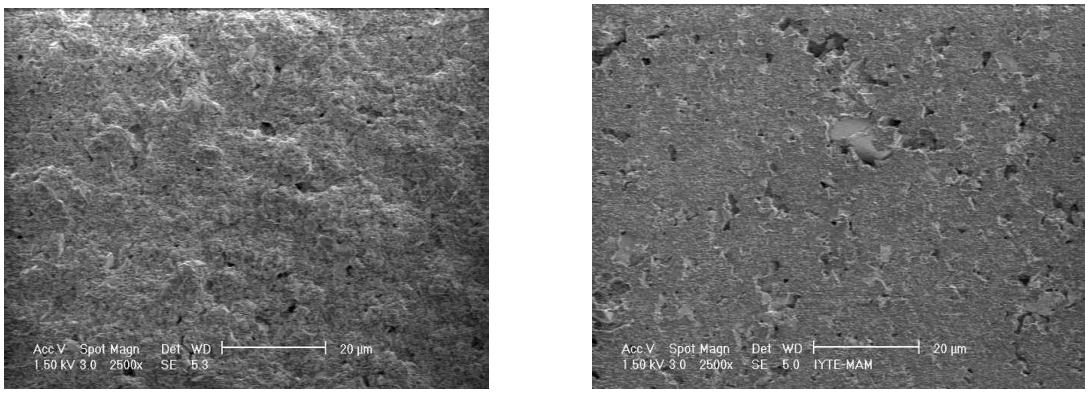

(a) (b)

Figure 5.7: Surface micrographs of the paint having 20% binder at 2500 magnification; (a): opaque side, (b): glossy side.

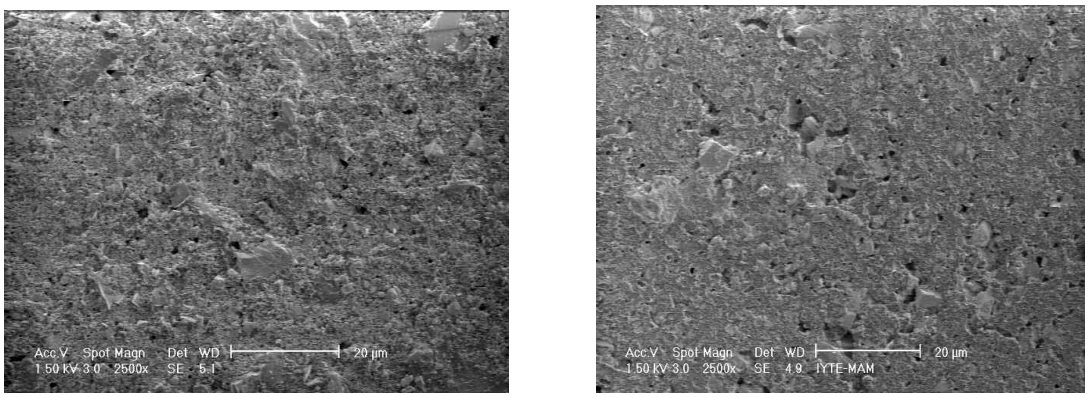

(a) (b)

Figure 5.8: Surface micrographs of the paint having 10% binder at 2500 magnification; (a): opaque side, (b): glossy side.

When micrograph of opaque and glossy sides are compared with each others, it was seen that the relatively high roughness of the opaque sides is obvious for all of the paint films. Another important result can be obtained by comparing the surface micrographs of the paint films with each others as shown in Figures 5.9a through 5.9d. According to these micrographs the paint having 40% binder almost have a non porous structure. When the binder amount in the paints decrease from 40% to 10%, more porous structure was observed in the films and this situation can be observed from both glossy and opaque sides of the films. It is well known that porous structure formation is a result of the pigment flocculation caused by insufficient wetting of pigments by the binder.

Figure 5.9 shows that in the paint having 40% binder, there is a matrix structure on which the pigments and other fillers exhibit relatively homogeneous distribution. However, as binder percentage decreases, pigment distribution becomes nonhomogeneous. Especially in paints having 20% and 10% binder, pigment flocculation and related to that some pores formed can be clearly seen. From the same figure it can be seen that although micro structure of the all paint films exhibit differences, it is difficult to distinguish the paint structures having 40% and 30% binder and also paints having 20% and 10% binder are similar. The remarkable difference in paint structures is observed when the binder amount is reduced from 40% to 20%.

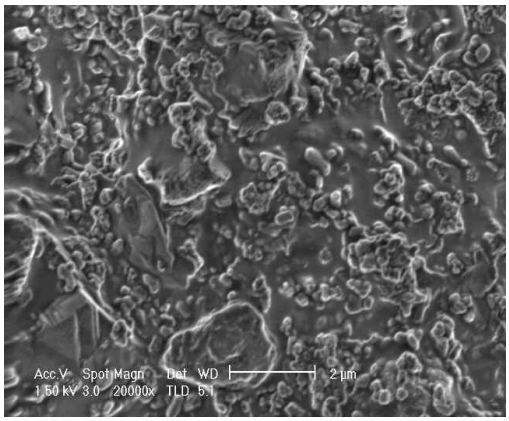

(a)

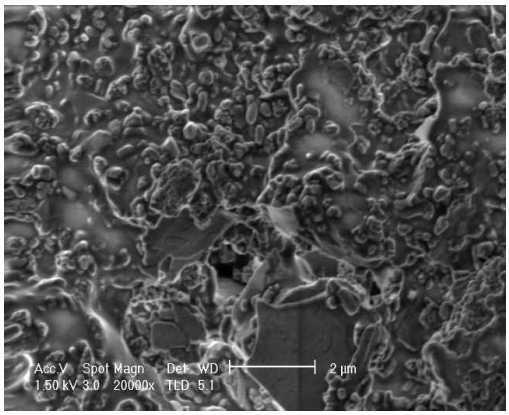

(b)

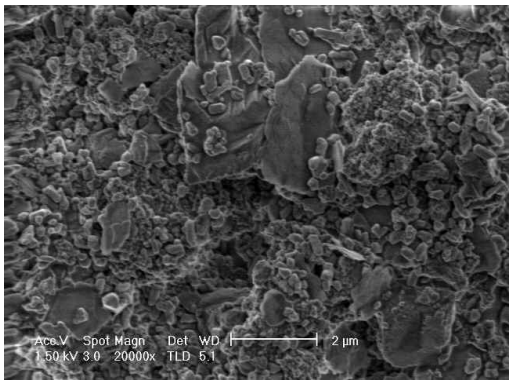

(c)

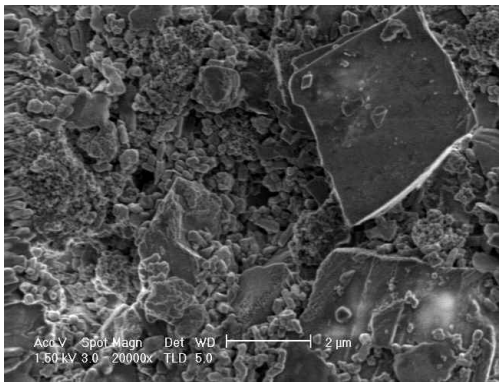

(d)

Figure 5.9: Surface micrographs of the paint films taken from opaque sides at 20000 magnification for the paint films having; (a): 40%, (b): 30%, (c): 20%, (d): 10% binder.

In the micrographs of the films taken by using BS detector, the compositional contrast give a good visual distinction between the copolymer matrix, pigments and pores contained in the paint films. As it is known that, the light regions in the micrographs show the heavier molecules and the dark regions show the lighter molecules. Also black regions seen in the graphs are attributed to the presence of the pores. Surface micrographs of each paint film taken at BS mode are shown in Figures 5.10 through 5.13. The presence of white regions in each graph indicates titania molecules in the structure.

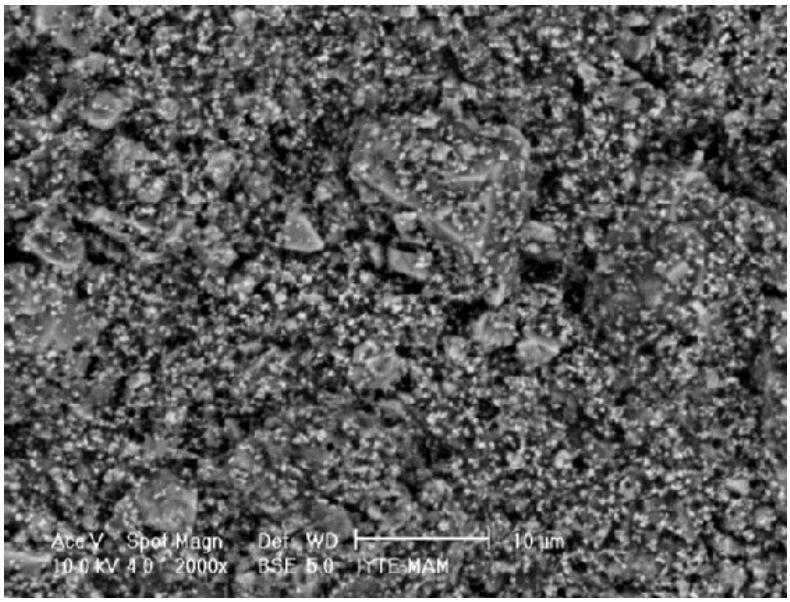

Figure 5.10: Surface micrographs taken at BS mode for the paint film having 40% binder at 2000X magnification.

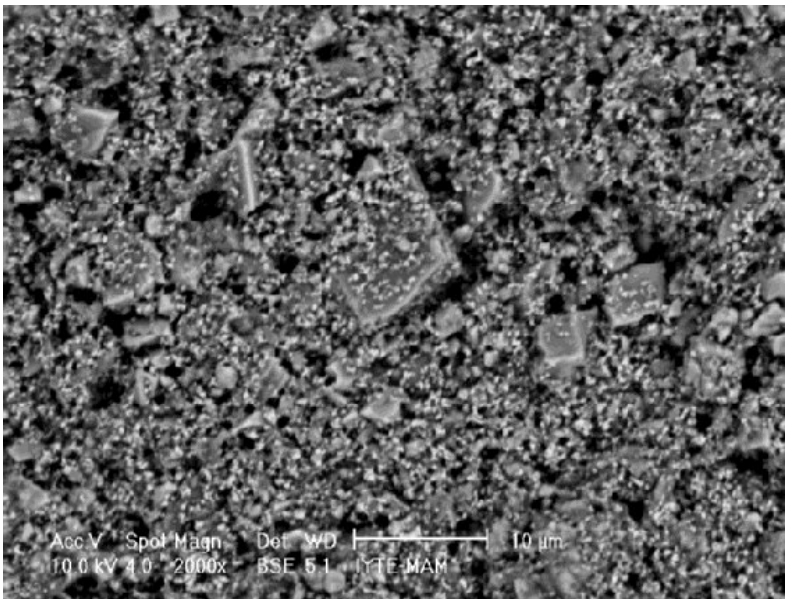

Figure 5.11: Surface micrographs taken at BS mode for the paint film having 30% binder at 2000X magnification.

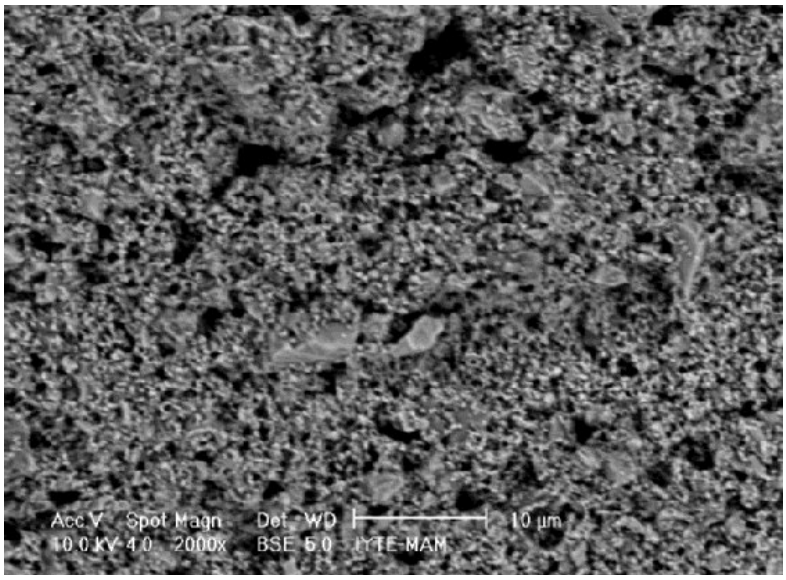

Figure 5.12: Surface micrographs taken at BS mode for the paint film having 20% binder at 2000X magnification.

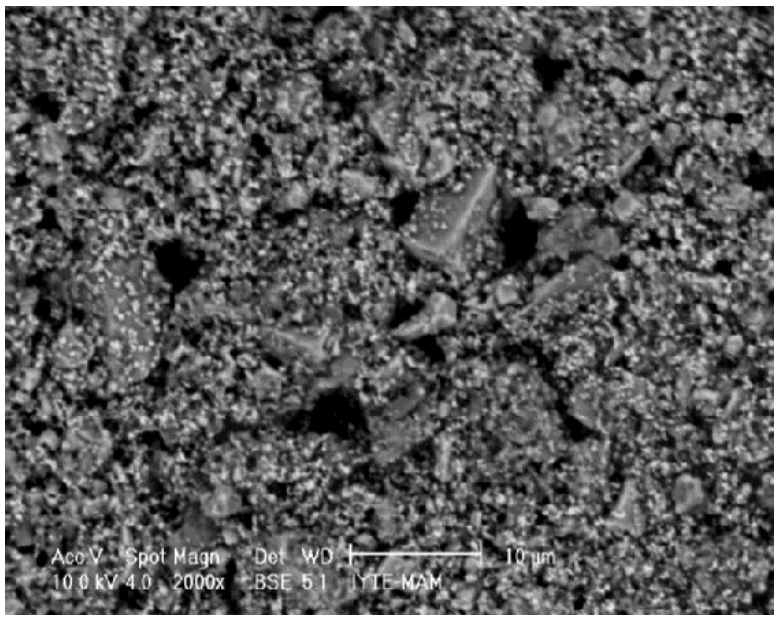

Figure 5.13: Surface micrographs taken at BS mode for the paint film having 10% binder at 2000X magnification.

5.1.3 Fourier Transform Infrared Spectroscopy Analysis

Figures 5.14 through 5.17 show that FTIR spectrums of the each paint film do not exactly overlap with each others but there are many common peaks. These are characteristic peaks expected from the methylmethacrylate-co-butylacrylate copolymer and some pigments added to the paint.

Common peak ranges at the spectrum are as follows:

3600-3060 cm^{-1}: OH group is observed due to the presence of water. In addition, C-H streching vibrations absorb in between 3000-2900 cm^{-1}.

1797.53 cm^{-1}; 1751.24 cm^{-1}: All saturated esters have strong sharp absorption peak at about 1740 cm^{-1} due to the C=O streching mode.

1720.39-1635.52 cm^{-1}: Liquid H_2O absorbs near 1640 cm^{-1}. In acrylates and methacrylates C=O absorb at 1725 cm^{-1}.

1260-1000 cm^{-1}: In the paint films this range corresponds to strong Si-O bands. It is known that silica absorbs near 1100 cm^{-1} .

700-500 cm^{-1}: TiO_2 has its strongest bands in the 700-500 cm^{-1} region and all paint samples gave peaks between these wavelenghts (Colthup et al., 1990).

Vitala et al. (2000) studied the morphology, microstructure, and chemical composition of pure and Ca and P doped TiO_2 films. They reported that TiO_2 show a strong broad absorption band in the region 1000-400 $cm^{-1}$and this bands correspond to the formation of Ti-O-Ti bonds. In their spectra the bands between 600-450 cm^{-1} was attributed to the amorphous TiO_2. Burgos and Langlet (1999) mentioned about the TiO_2 sol-gel reactions and in IR studies they found bands belonging to Ti-O and Ti-O-Ti groups in the range of 800-400 cm^{-1}. All paint films used in this study exhibit absorbtion bands between the values mentioned above, which confirm the presence of TiO_2.

Reig et al. (2002) proposed constant ratio method for the quantitative analysis of calcite and quartz in geological samples. They reported that calcite is one of the three crystalline forms of calcium carbonate, the other ones are aragonite and vaterite, and all of these crystal minerals are represented by the same chemical formula but do not exhibit same infrared spectrum. Although there are three types of calcium carbonate crystal, the most commonly seen form of calcium carbonate is calcite. In their article FTIR spectrums of calcite is given as 1420, 875 and 712 cm^{-1}. The band which represent the silica was reported as 798 and 779 cm^{-1} and stated that quartz is one of the minerological forms of the silica and there are large amount of quartz in the nature. Sönmez and Cebeci (2003) stated that IR bands at 854.4 and 875.6 cm^{-1} are characteristics of the carbonate in calcite.

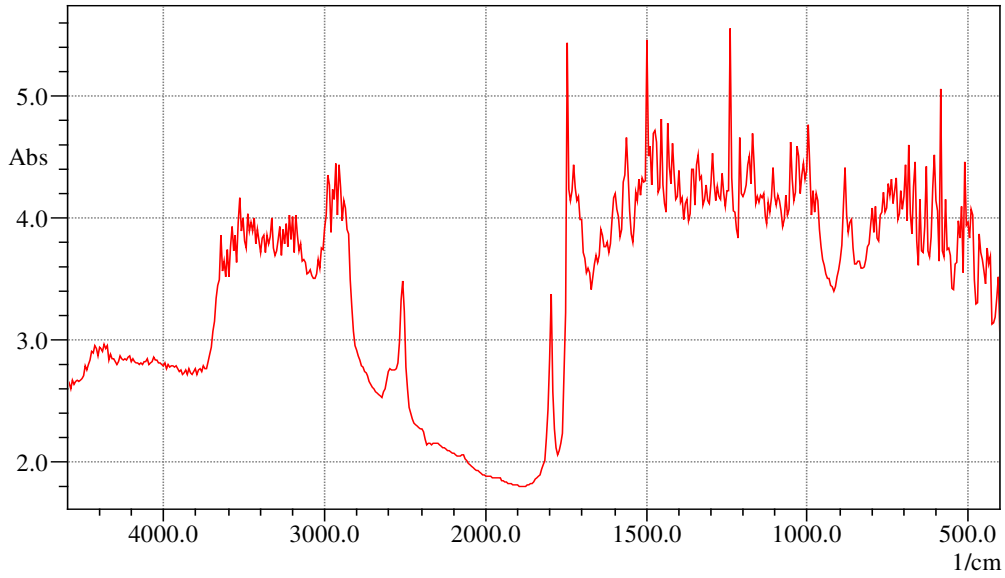

Figure 5.14: FTIR spectrum of the paint film having 40% binder.

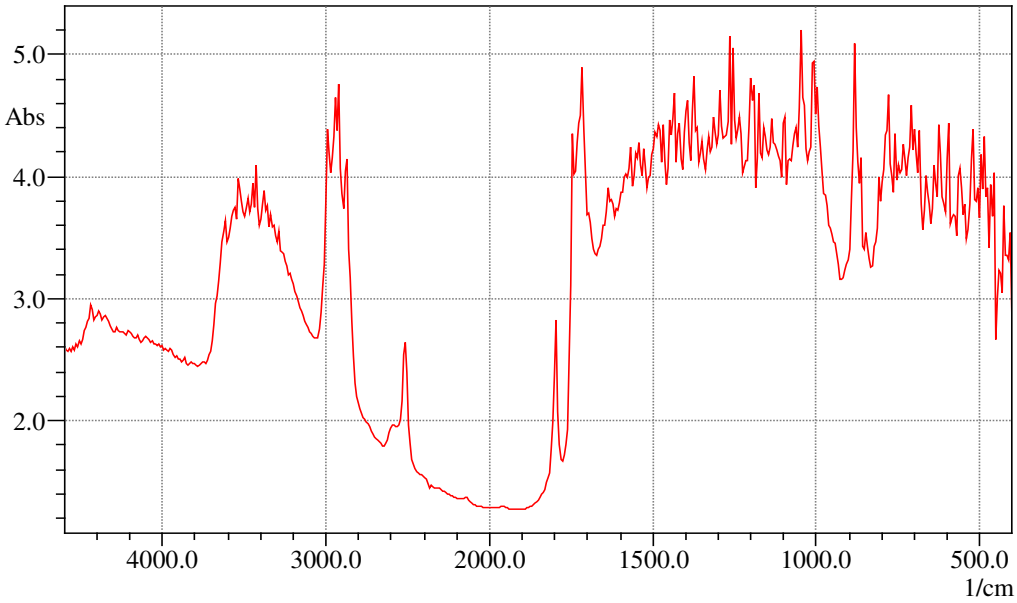

Figure 5.15: FTIR spectrum of the paint film having 30% binder.

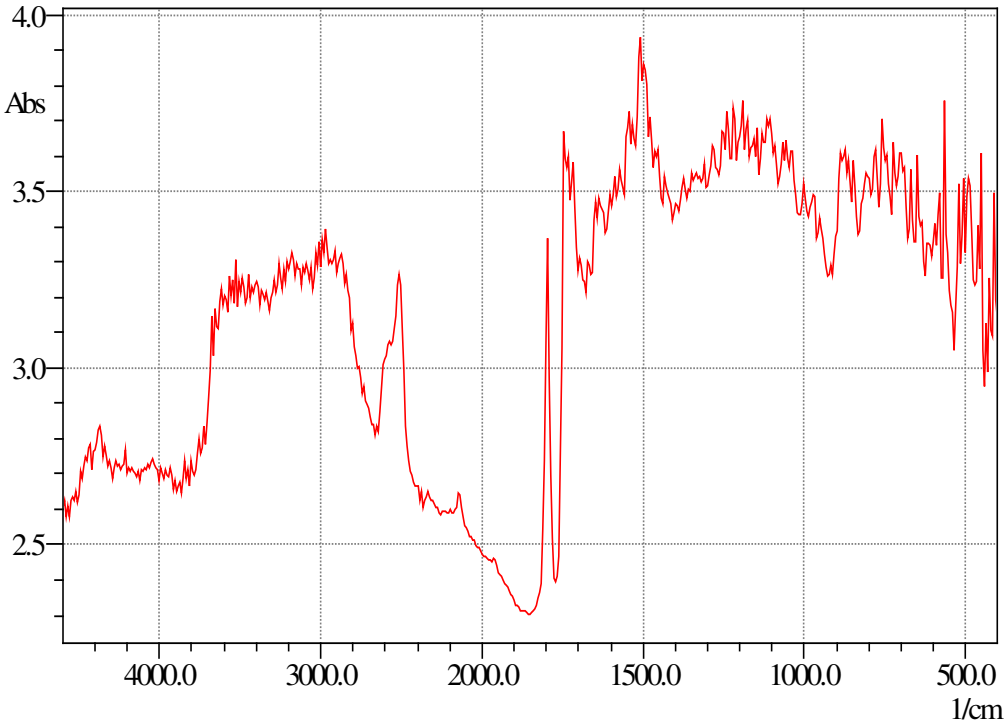

Figure 5.16: FTIR spectrum of the paint film having 20% binder.

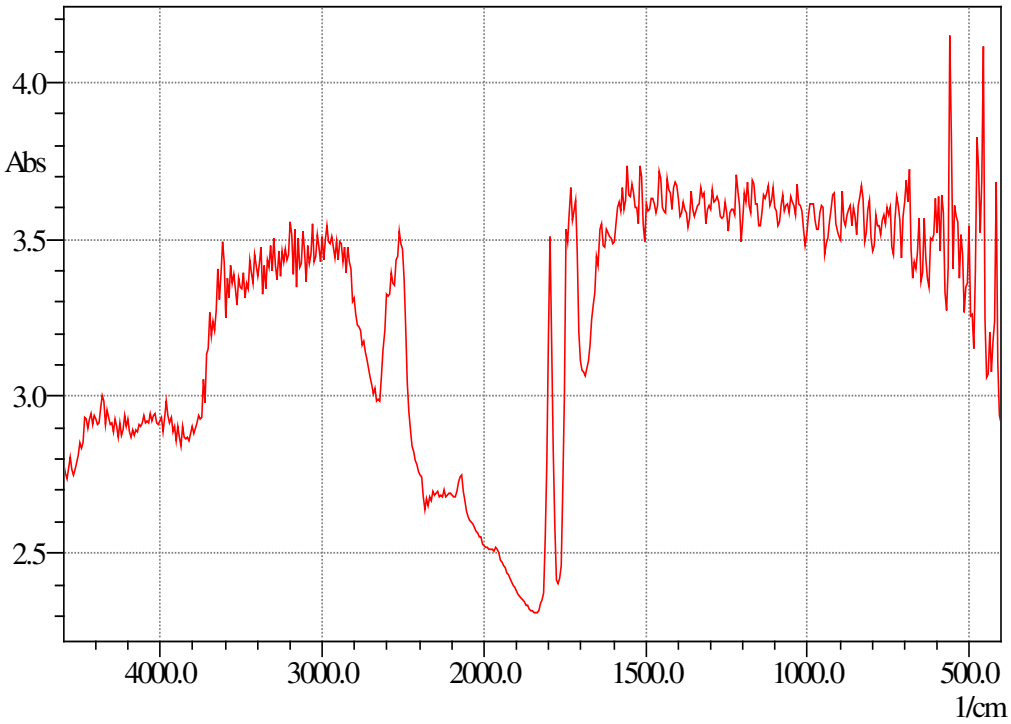

Figure 5.17: FTIR spectrum of the paint film having 10% binder.

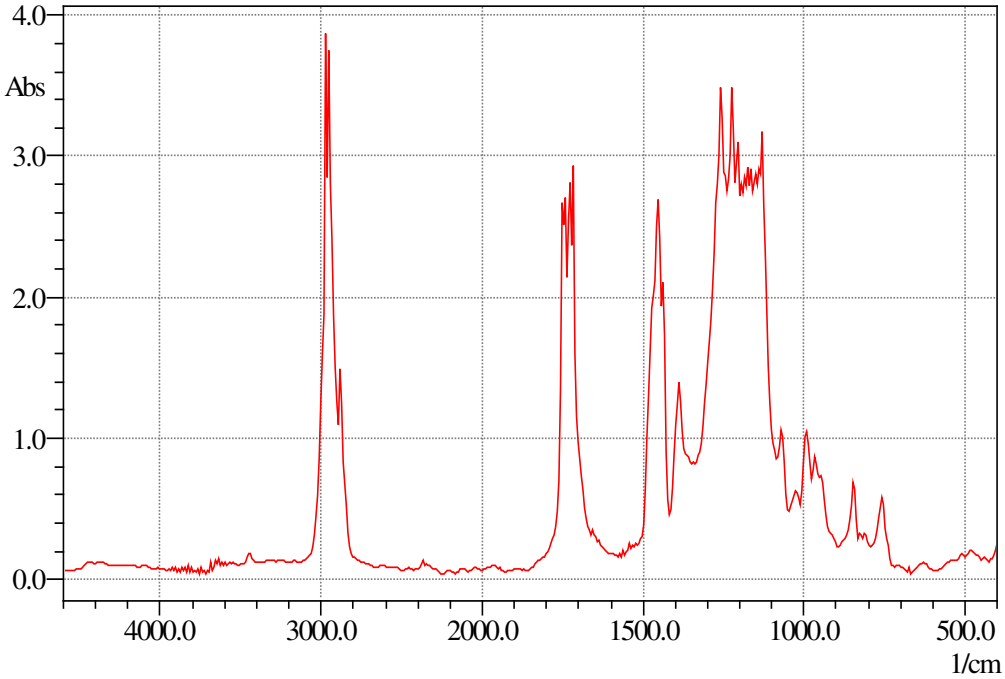

Figure 5.18: FTIR spectrum of the pure copolymer.

5.1.4 Elemental Composition of the Paint Films

EDX results were obtained for each paint film by analysing randomly selected 20 different points over their opaque sides and results were evaluated by taking average of the values collected from these points. Average weight percent of elements present in the paint films are represented in Table 5.2. According to the EDX results the common elements seen in each film are carbon, oxygen, titanium, calcium, silicon, aluminium, magnesium, and sodium. The average amount of carbon element decreases as the binder percentage decreases, however, oxygen amount remains nearly the same. According to the X-ray analysis results, all elements except oxygen and carbon are found as oxygen containing compounds in the paint, while carbon is only seen in calcite besides binder material. Since these oxygen containing elements are found in a significant amount in the paint having 10% binder, it is not surprising to see relatively high amount of oxygen and low amount of carbon in this paint.

Table 5.2: Average weight percent of elements present in the paint films.

Binder (%)	C	O	Na	Mg	Al	Si	Ca	Ti
40	50.3	37.4	0.7	0.9	1	3.2	2.7	3.8
30	45.2	40.9	0.8	1	1.1	3.8	3.4	3.8
20	41.6	42.3	0.7	1.1	1	3.3	4.3	5.7
10	26.9	42.2	0.9	1.3	1.5	5.2	9.4	12.5

5.1.5 Map of the Paint Films

In Figures 5.19 through 5.22 map diagrams of the paint films are shown. According to these figures map diagrams belonging to 40% and 30% binder indicate relatively homogeneos distribution of elements. Especially in the paint having 40% binder a homogeneous distribution is very remarkable. In paint having 30% binder calcium element which is represented by blue colour exhibits some flocculations in some regions. The formation of flocculations in silicon and calcium elements in the paint having 20% binder is very obvious. The most heterogeneous distribution of elements is observed in the paint having 10% binder, as shown in Figure 5.22.

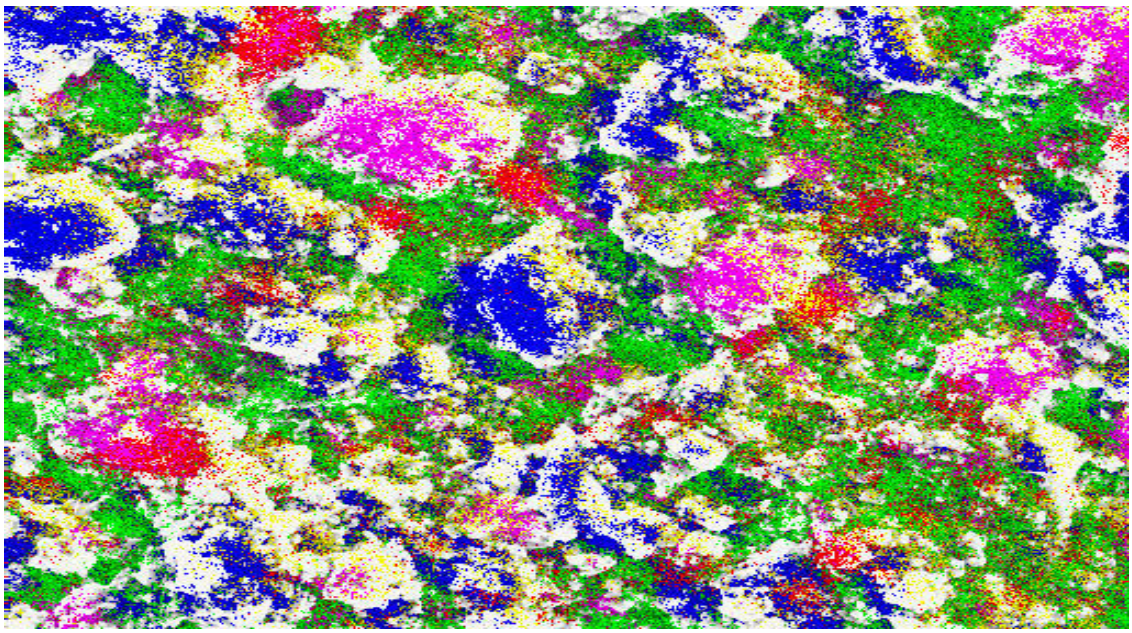

Figure 5.19: Map of the paint film having 40% binder at 2000X magnification; blue: calcium, green: titanium, magenta: silicon, yellow: oxygen, red: magnesium, white: carbon.

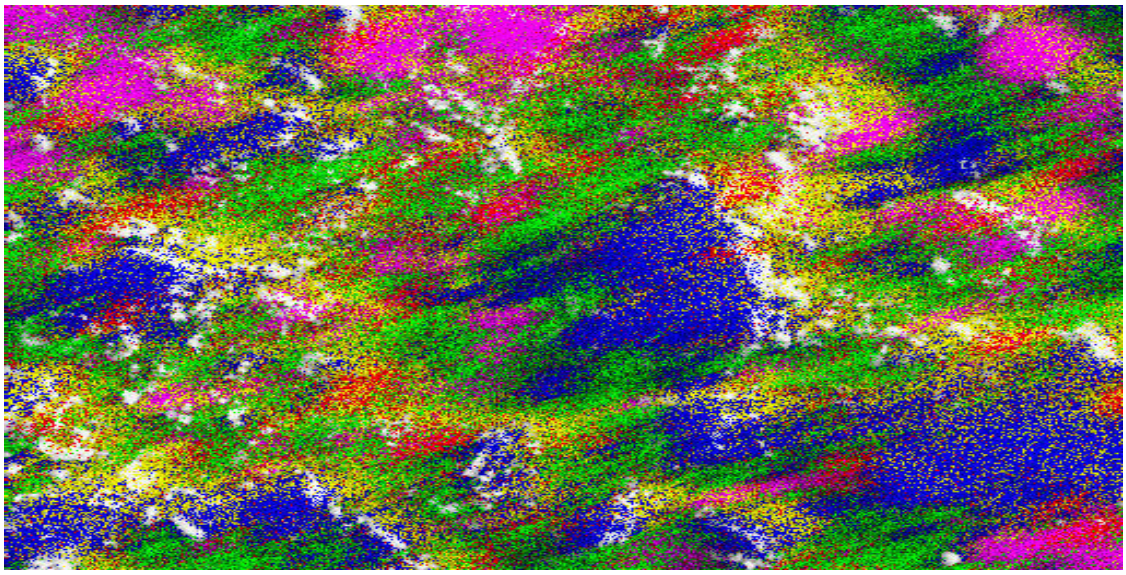

Figure 5.20: Map of the paint film having 30% binder at 2500X magnification; blue: calcium, green: titanium, magenta: silicon, yellow: oxygen, red: magnesium, white: carbon.

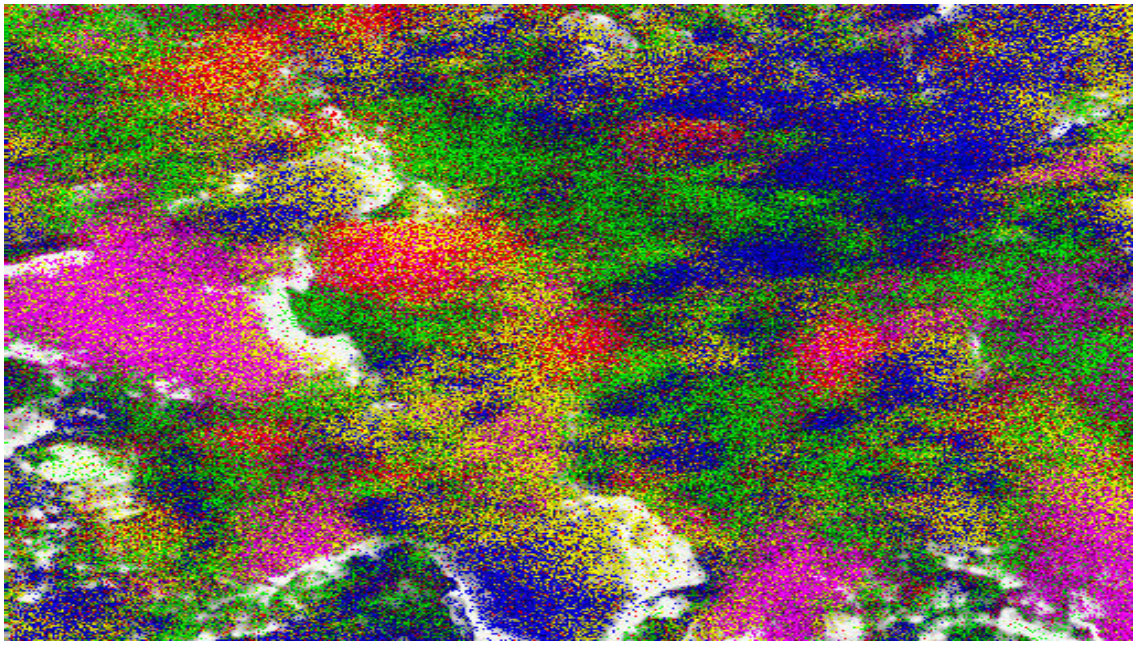

Figure 5.21: Map of the paint film having 20% binder at 3500X magnification; blue: calcium, green: titanium, magenta: silicon, yellow: oxygen, red: magnesium, white: carbon.

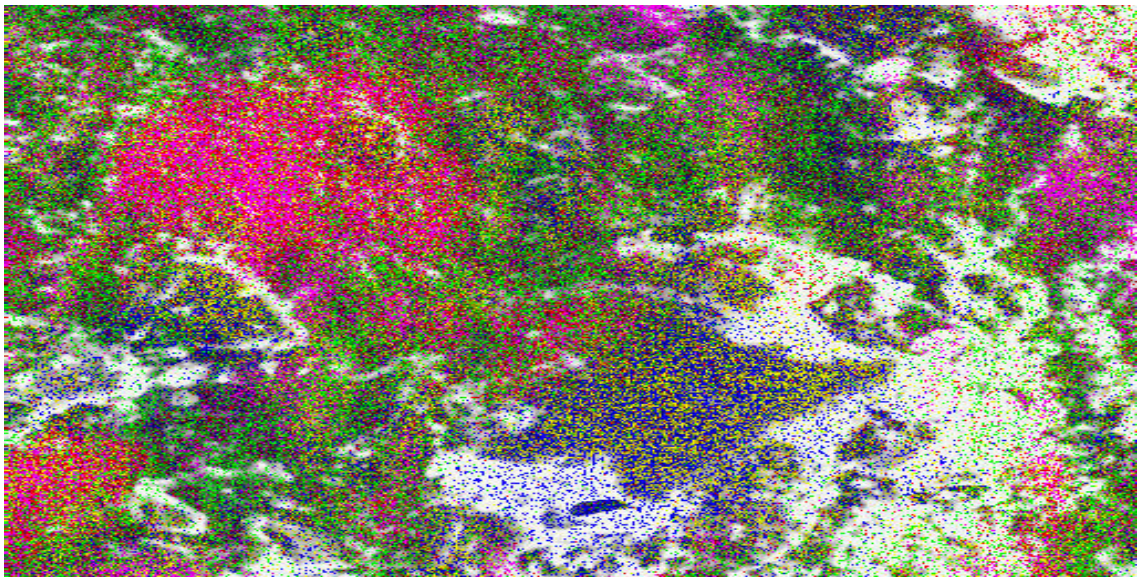

Figure 5.22: Map of the paint film having 10% binder at 5000X magnification; blue: calcium, green: titanium, magenta: silicon, yellow: oxygen, red: magnesium, white: carbon.

5.1.6 Roughness of the Paint Films

The roughness of the paint films was measured using Atomic Force Microscope in contact mode. For this purpose, each paint film was scanned at five different surfaces over 100 µm x 100 µm areas. According to the AFM results, the average overall roughness of the paint films having 40%, 30%, 20% and 10% binder are 133.8, 124.7, 144.3 and 144.3 nm, respectively in terms of Ra values. Here Ra, the height variance of the line/surface, corresponds to the following expression (Cannon and Pethrick, 2002).

$$\frac{1}{n}\sum_{i}^{n}\left|Z_i - Z_{avg}\right| \qquad (5.1)$$

5.1.7 Thermal Analysis

Figures 5.23 and 5.24 show the TGA curves of the paint films and pure copolymer film, respectively. According to these results, degradation process of the paint films occur at two steps, whereas the thermal degradation of the pure copolymer film occur at one step. Another difference in the degradation mechanism of the paint films and pure copolymer is that at the end of the degradation process all paint films left

thermally stable char. However, pure copolymer film degraded until losing all of its mass, a thermally stable char was not observed. In Table 5.3, degradation temperatures of the films and mass losses are summarized. It is seen that if the binder amount in the paint decreases, the total mass loss of the paint decreases.

Table 5.3: Degradation temperature and mass loss of the films.

Sample	Total mass loss (%)	First step mass loss (%)	Second stepmass loss (%)	T_{onset} of first step (^oC)	T_{endset} of first step (^oC)	T_{onset} of second step (^oC)	T_{endset} of second step (^oC)
40% binder	47.51	26.36	24.49	257.4	411	667.1	776.2
30% binder	43.67	21.22	24.24	258.3	409.2	668.9	775
20% binder	39.82	15.38	24.94	269.4	400.3	663.8	776.3
10% binder	34.88	9.21	24.89	276.2	400.1	661.7	785.7
Pure binder	99.18	-	-	263.6	599.9	-	-

Mass loss in the first step is associated with the decomposition of the binder material, methylmethacrylate-co-butylacrylate. Thus, in this step when the binder amount in the paint films decreases, mass losses decreases and the temperature range of the degradation process becomes narrow. For pure copolymer the temperature range for the degradation process is large compared to the paint films since in this case the sample contains 100% binder. The second step mass loss is attributed to the degradation of calcite into calciumoxide and carbondioxide by the following reaction.

$$CaCO_3(s) \longrightarrow CaO(s) + CO_2(g) \qquad (5.2)$$

At the end of second step mass loss, the residual thermally stable char contains CaO and titania which are both stable over 1000 ^oC.

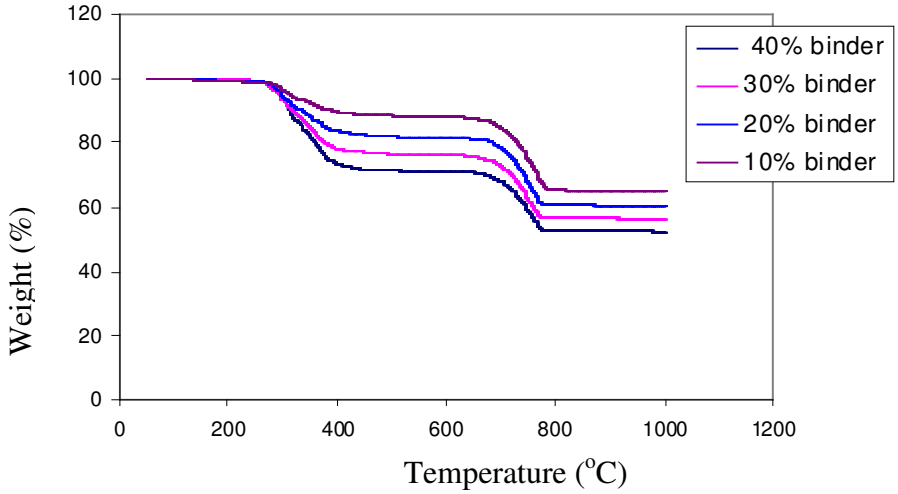

Figure 5.23: TG curves of the paint films.

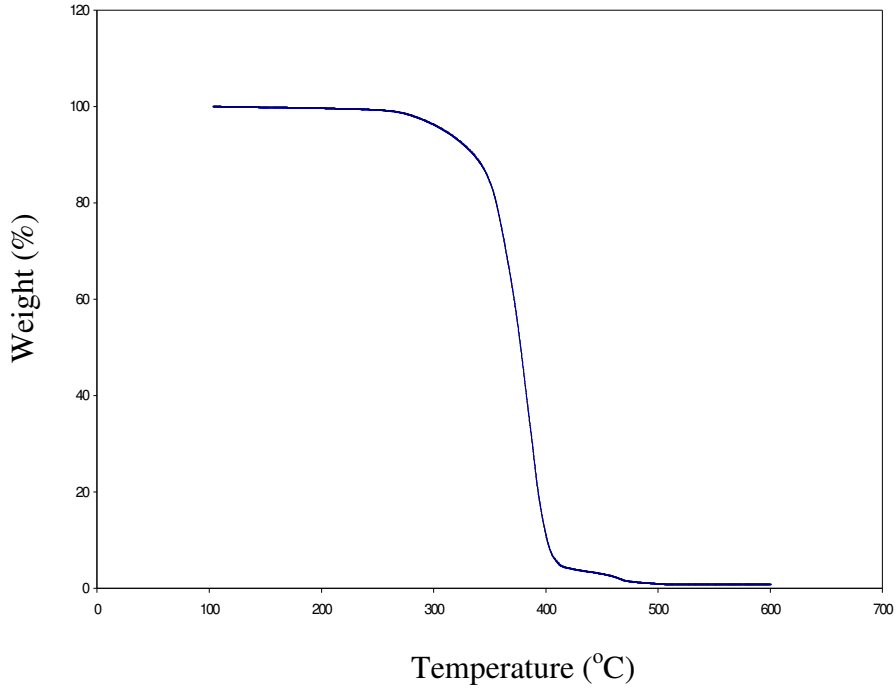

Figure 5.24: TG curve of the pure copolymer.

5.1.8 Differential Scanning Calorimetry Analysis of the Paint Films

Figures 5.25 through 5.29 show the DSC curves of the paint and pure copolymer films. According to these curves, paint films exhibit two exothermic decomposition peaks while the pure copolymer exhibits a single decomposition peak. During the decomposition of the paint films, heat is released due to the thermal oxidation of the

organic fractions. However, in the case of pure copolymer degradation process is endothermic since the oxygen content in the structure of pure copolymer is not enough to initiate the decomposition.

During the DSC analysis, glass transition temperatures of the paint films were determined as 34.14 ^{o}C, 34.11 ^{o}C, 32.82 ^{o}C and 33.96 ^{o}C while the glass transition temperature of the pure copolymer was found as 31.67 ^{o}C. These results suggest that addition of pigments, fillers and other additives does not significantly influence the glass transition temperature of the paint films. This situation may be caused due to the weak interaction between the pigments and the acrylic binder. Similar result was reported by Perera (2004). To determine enthalpy of the thermal degradation process, the area under the whole exotherm was integrated and the results are summarised in Table 5.4. Experimental data for the four different paint films were then gathered in Figure 5.30, plotting measured ΔH (kJ/kg) vs % binder content. The results show a good correlation of heat output with polymer concentration. Thus, it appears that determination of heat output from thermal decomposition of organic fraction in the paint by using DSC may be used to estimate binder concentration in the paint films.

Table 5.4: Decomposition peak temperatures and heat of decomposition of the binder.

Sample	T_{onset} (^{o}C)	T_{endset}(^{o}C)	ΔH (kj/kg)
40% binder	214.1	498.5	364.5
30% binder	220.1	477.8	271.4
20% binder	226.8	494.1	182.9
10% binder	233.3	499.9	107

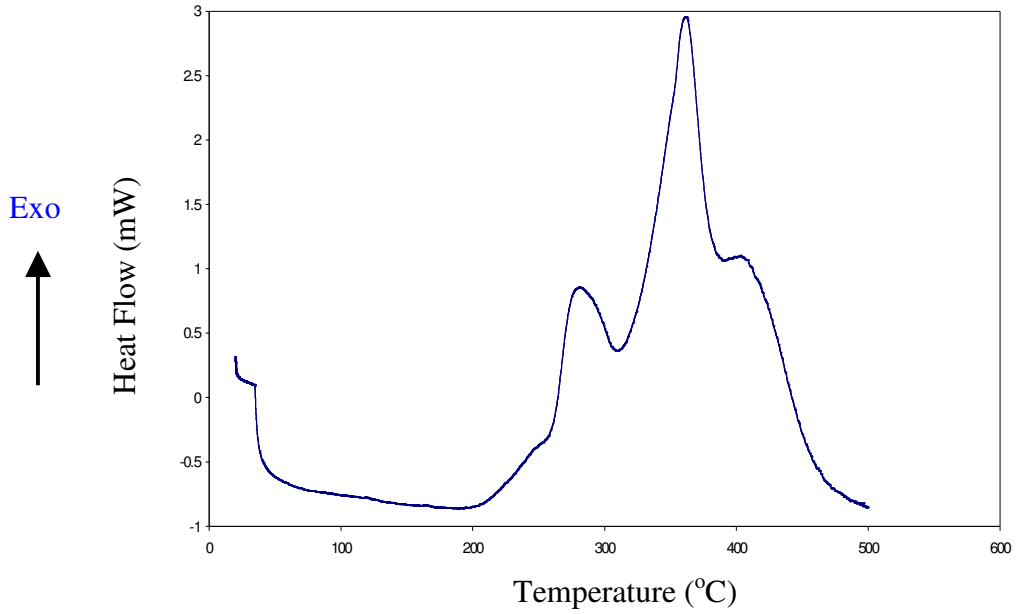

Figure 5.25: DSC curve of the paint film having 40% binder.

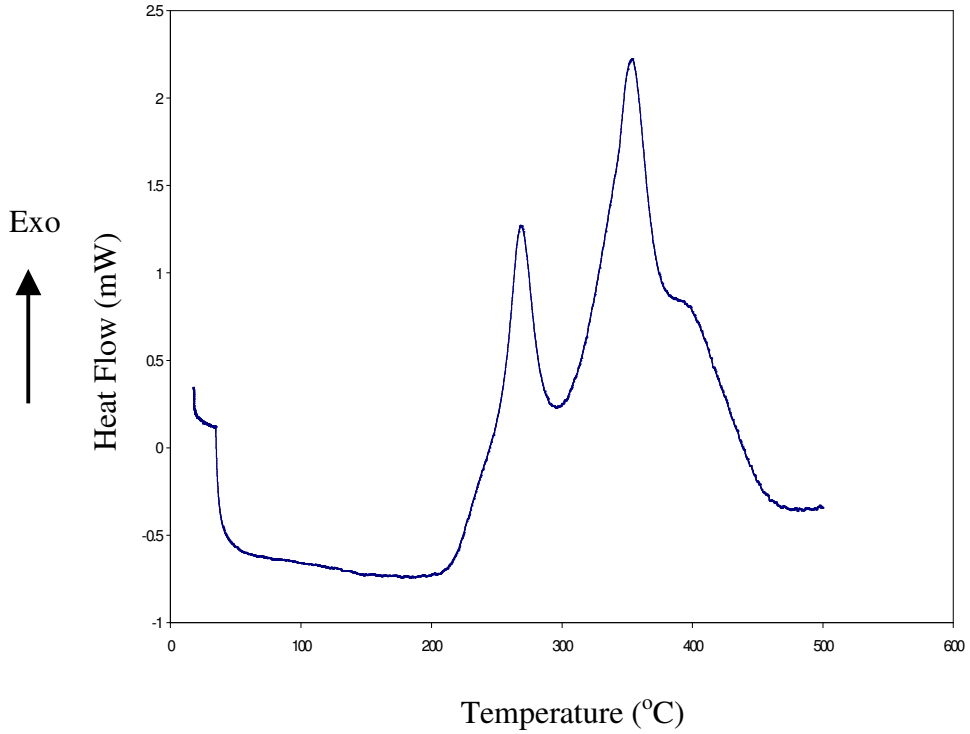

Figure 5.26: DSC curve of the paint film having 30% binder.

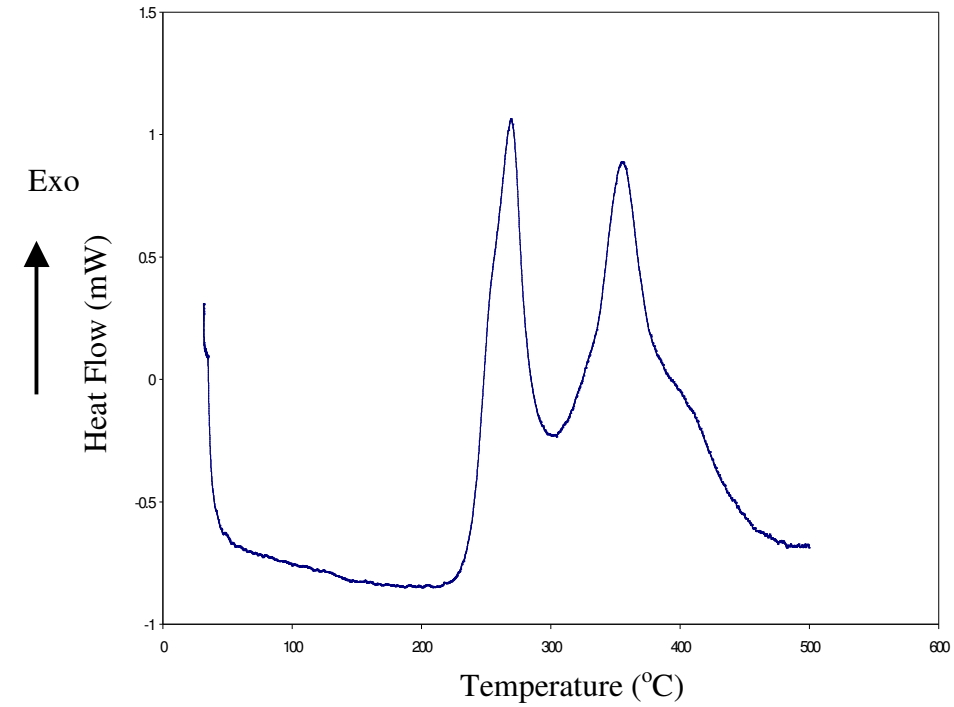

Figure 5.27: DSC curve of the paint film having 20% binder.

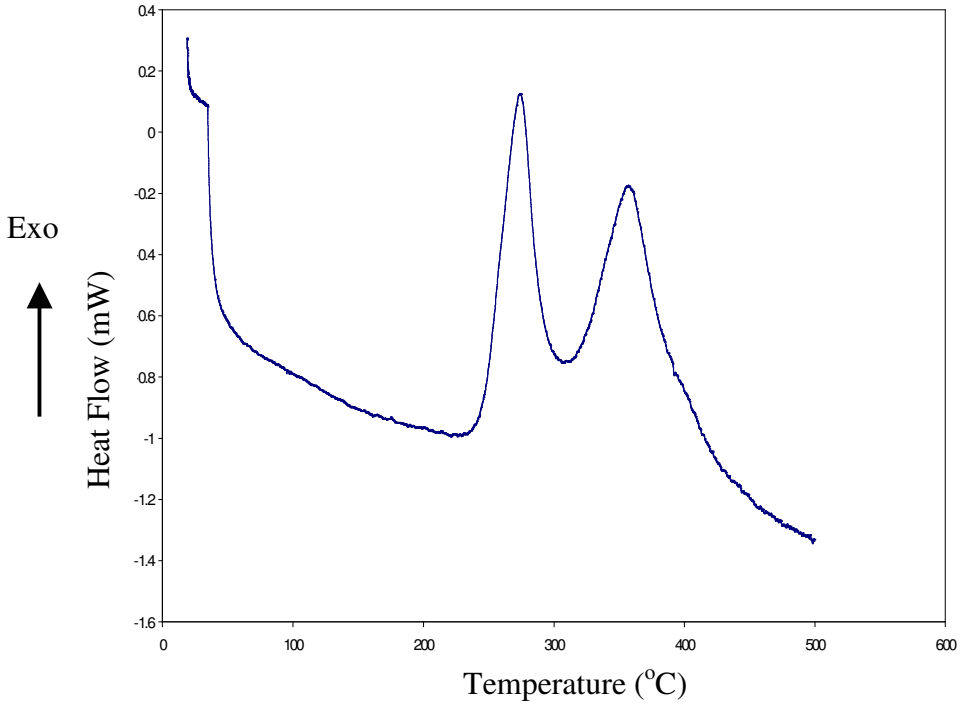

Figure 5.28: DSC curve of the paint film having 10% binder.

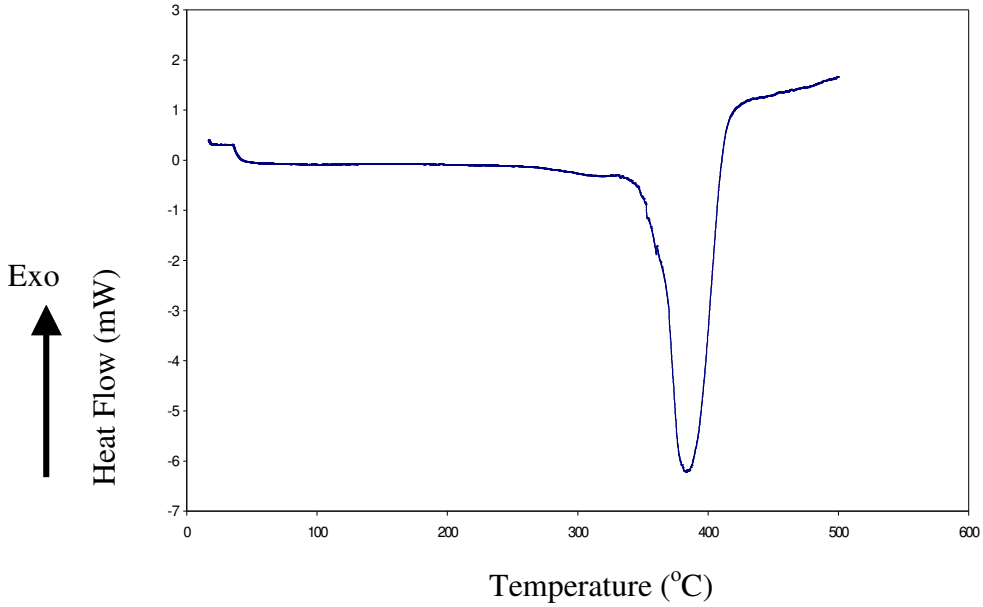

Figure 5.29: DSC curve of the pure copolymer.

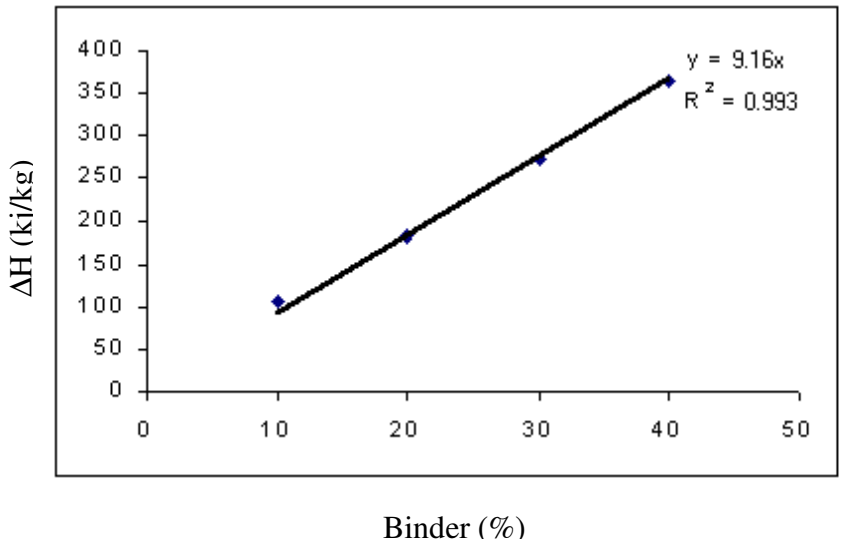

Figure 5.30: Heat of decomposition as a function of binder content.

5.1.9 X-Ray Results

At the end of the EDX analysis, the elements in the paint films were determined and they were listed in Table 5.2. X-Ray analysis was used to determine form of these elements. This analysis showed that all paint films gave nearly the same spectrums as shown in Figure 5.31. According to the X-ray diffraction analysis, calcium is in the form of calcite ($CaCO_3$) as expected which is a compound generally used as a filler in

the paint and give white colour to the paint. The crystalline peaks of this compound are observed at $^{o}2\theta$ = 23.2, 29.5, 31.5, 36, 39.5, 43.2, 47.2, 47.5, 48.5, 56.5, 57.5, 58.2, 60.8, 61, 61.5, 63.1, 64.8, 65.6, 69.2. These values are compatible with the study of Jeoung-Ah (2004). In that study, microstructure and chemical compositions of paper composite porcelain was characterized by using XRD and SEM techniques. Titanium is in the form of titania (TiO_2) and gave peaks at the $^{o}2\theta$ angles of 27.5, 36, 39.3, 41.3, 44.2, 54.5, 56.7, 62.8, 64.1, 65.7, 69.1, 69.8. It is one of the commonly used pigments in the paint industry and gives white colour like calcite but it is more expensive than calcite. For this reason instead of titania, calcite is preferred, but the amount of calcite should not exceed certain level since calcite does not meet all the requirements offered by the titania (Tiarks et al., 2003).

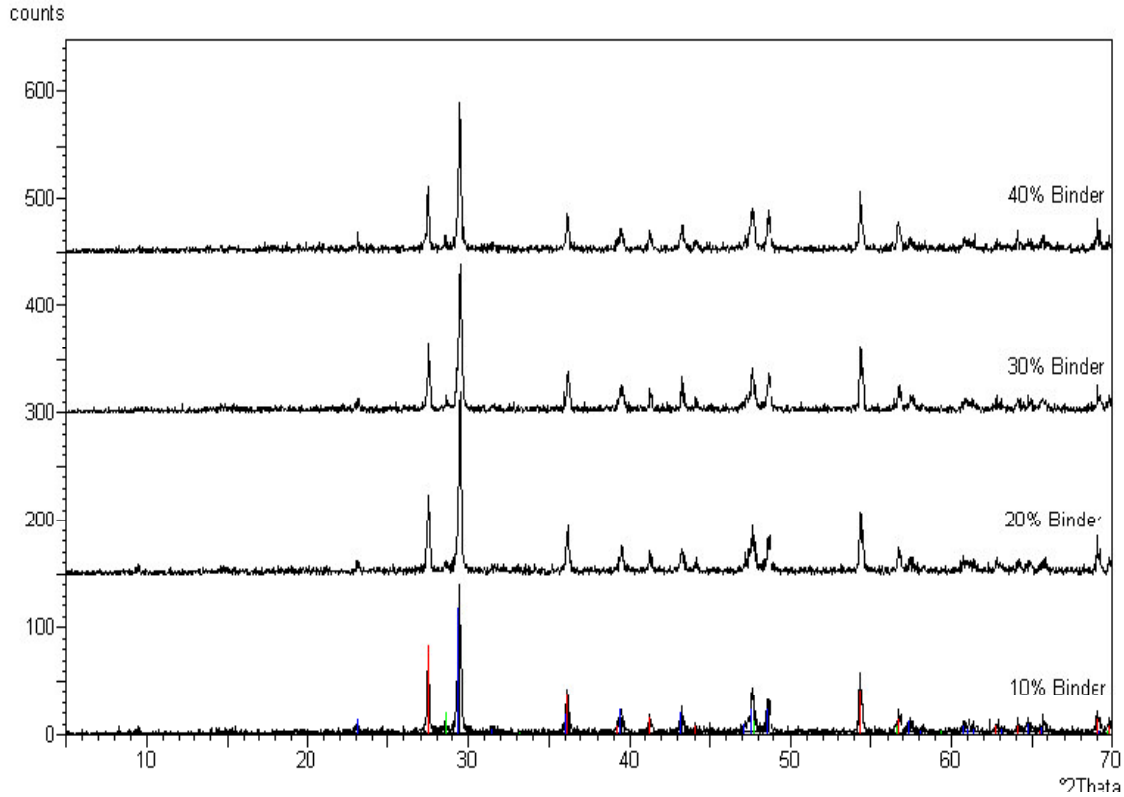

Figure 5.31: X-ray diffraction diagram of the paint films

5.2 Solid-Liquid Ratio of the Samples

In Table 5.5, the weight losses due to the evaporation of water from the samples after each drying process were represented. According to the table, the most significant loss at the end of the first drying belongs to the pure copolymer. As it is determined in Table 5.5, after the evaporation of the water the remaining solid ratios of the samples are very close to each others. As an average the samples lost their water content at a percentage of 26.5 % at the end of the drying process.

Table 5.5: Mass loss values of the samples after the first and second drying processes.

Sample	Mass loss at 70 ^{o}C (%)	Mass loss at 80 ^{o}C under vacuum (%)	Total mass loss (%)	Remaining solid at the end of the drying processes(%)
40 % binder	13.4	17	28	72
30% binder	15.4	14.4	27.6	72.4
20 % binder	21.5	4.8	25.3	75
10 % binder	20.9	5.2	25	75
Pure binder	35.36	-	-	-

For the paints having 40% and 30% binder, total mass lost is almost equally shared between the drying steps. However, paints having 20% and 10% binder mainly lost their masses after the first step. This is due to the fact that in the paints with higher binder content diffusional resistance to transport of water and other volatile components is larger than that in paints with lower binder content.

5.3 Permeation Studies

Permeation studies were carried out to determine water vapour permeability coefficient of pure copolymer and the paint films with binder contents of 40%, 30%, 20%, 10%. In addition to deionized water, 2.9% wt and 5% wt NaCl solutions were used as solutes in order to simulate rain conditions. Permeation experiments using deionized water as a solute were performed by exposing the sides of the paint films to deionized water. The films were reversed to see the effect of surface structure on the permeability coefficient. When NaCl is used as the solute, only smooth and glossy sides of the films were exposed to the feed (solute) source. The thickness of films used in the

experiments are different from each others, thus the change of relative humidity in the upper compartment was plotted as a function of time normalized with the thickness of the films as illustrated in Figures 5.32 through 5.34. Permeability coefficient of water vapour was calculated from the slope of linear portion of $\ln\frac{P_{1L}-P_{1ui}}{P_{1L}-P_{1u(t)}}$ vs time graph and the results were tabulated in Table 5.6. When the binder amount decreases, permeability coefficient of the paint films increases with the increase in the porosity of the films as shown by SEM pictures in Figures 5.10 through 5.13. Pore formation in the films is associated with pigment flocculation due to insufficient wetting of the pigment particles by the binder. The permeability coefficient of the pure copolymer is very close to that of the paint film with the binder content of 40%, since this paint film contains a relatively homogeneous and nonporous structure, similar to the structure of the pure copolymer film. An insignificant difference in permeability coefficients was observed for the paint films having 40%, 30% and 20% binder when their opaque and glossy sides were exposed to water vapour. However, for the paint film containing 10% binder, permeability coefficient is almost two times higher when its glossy surface was exposed to the water vapour. This result can be explained by the difference in roughness of the surfaces. In AFM, the roughness of the glossy surfaces were determined while measurements could not be taken on opaque surfaces due to very high roughness values. When opaque side of the paint film is exposed to the feed source, water molecules first permeate through a much more rough surface, thus see a higher resistance to their transport at the beginning of the process. The increase in resistance to the permeation of water molecules causes smaller permeability coefficients since these values are determined from the data collected especially at early times of the permeation process. The largest overall roughness value was determined for the paint films with the binder contents of 20% and10%. Thus, the difference in permeability coefficients determined by exposing different sides to the water vapour is greatest for the paint film having 10% binder. It should be also noted that, the linear permeation model given by Equation (2.30) is valid for a longer time period for the pure copolymer and paint films containing 40% and 30% binder.

When NaCl solution was used as a solute, permeability coefficient of water vapour decreases for the pure copolymer and the paint films having 40%, 30% binder, since partial pressure of water vapour on the feed side, consequently, the concentration difference through the film decreases. An increase in permeability coefficients was

observed for the films with lower binder contents of 20% and 10%. As explained before, this is due to the fact that the validity of permeation model for these films is quite limited. Infact, as expected the increase in relative humidity of the upper compartment is lower when the surfaces of these films are exposed to NaCl solution. This can be seen by comparing Figures 5.32 and 5.34 which plot the change of relative humidity wih respect to normalized time.

Permeability coefficient of water in coatings/paint films strongly depends on the coating formulation which influence the final structure of the film. Hulden and Hansen (1985) reported the permeability coefficient of water in acrylic latex coating as 28.3×10^{-12} mol/s.cm.kPa. The paint films used in this study are also acrylic latex coatings and the value reported by Hulden and Hansen (1985) is close to the permeability coefficient of water in the paint film with the lowest binder content of 10%.

Table 5.6: Permeability coefficients of water vapour through pure copolymer and paint films which are in equilibrium with saturated vapour of deionized water and NaCl solutions.

Binder (%)	Deionized water (opaque side) $P_{eff} \times 10^{12}$ (mol/s.cm.kPa)	Deionized water (glossy side) $P_{eff} \times 10^{12}$ (mol/s.cm.kPa)	2.9 wt % NaCl (glossy side) $P_{eff} \times 10^{12}$ (mol/s.cm.kPa)	5 wt % NaCl (glossy side) $P_{eff} \times 10^{12}$ (mol/s.cm.kPa)
100	0.73	0.73	0.36	-
40	0.77	0.79	0.71	0.73
30	1.53	1.84	1.22	0.76
20	12.46	14.85	17.5	14.98
10	18.63	35.3	45.87	-

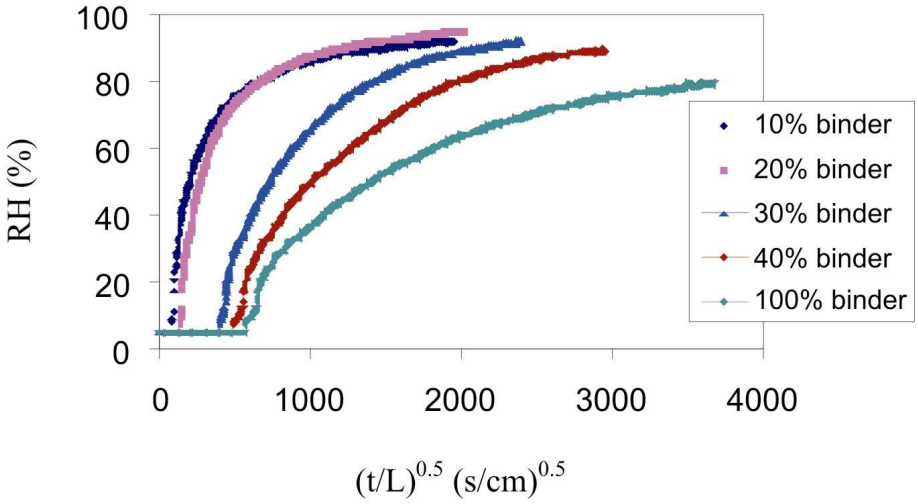

Figure 5.32: The change in relative humidity in the upper compartment when glossy sides of the films are exposed to deionized water vapour.

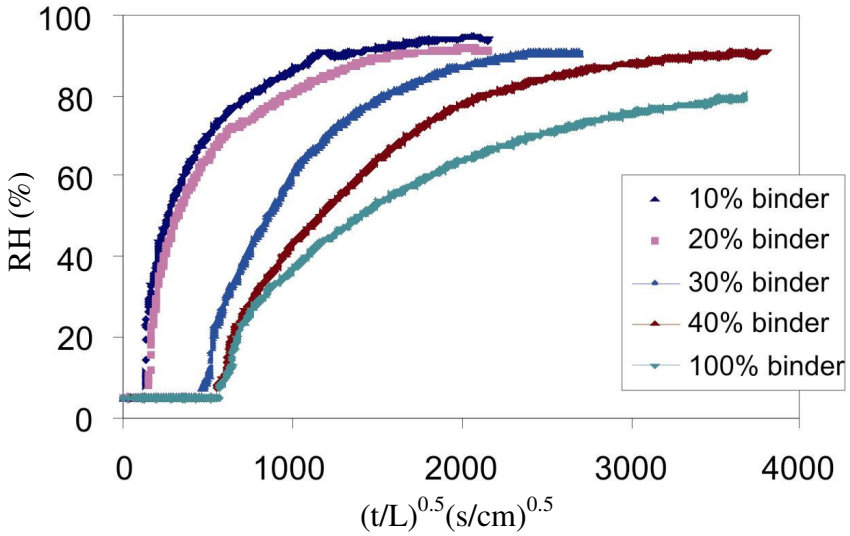

Figure 5.33: The change in relative humidity in the upper compartment when opaque sides of the films are exposed to deionized water vapour.

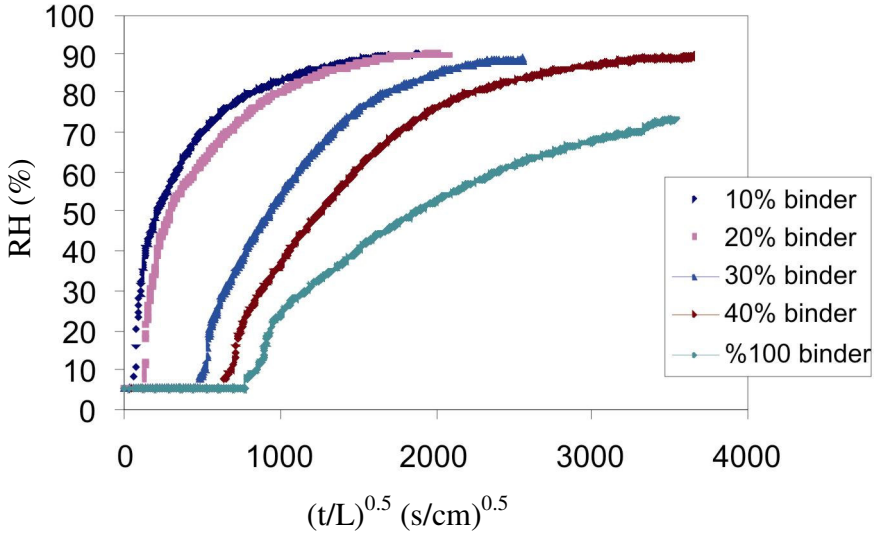

Figure 5.34: The change in relative humidity in the upper compartment when glossy sides of the films are in equilibrium with the water vapour of aqueous 2.9 wt % NaCl solution.

5.4 Equilibrium Isotherms

Figures 5.35 through 5.38 gives the vapour-sorption equilibrium data for water-paint systems. Volume fraction of water in the copolymer/paint was plotted against the activity of the water vapour calculated from Equation (5.3);

$$a_w = \frac{P_1^o(T_{water})}{P_1^o(T_{column})} \tag{5.3}$$

Experimental data shows that water sorption capacity of the paint films decreases as their binder content decreases indicating that water sorption in the paint films takes place in the binder fraction. This result is in accordance with the expectation since pigments are generally dense, inorganic compounds with hydrophobic nature.

Equilibrium isotherms of paint systems were successfully fitted by the Flory-Huggins thermodynamic theory and the Flory-Huggins interaction parameters, χ, for the paint films with the binder contents of 40%, 30%, 20% and 10% were found as 2.07, 2.07, 2.22, 2.61, respectively. All of the interaction parameters are greater than 0.5 indicating that water is not a good solvent for the paint films. Maximum water sorption capacity of the films, corresponding to activity equals to one, cannot be determined

experimentally due to condensation risc in the column when the temperature of the water vapour is equal to the temperature of the column. On the other hand, utilizing the Flory-Huggins thermodynamic theory these values were predicted as 6.4%, 6.4%, 5.28% and 3.3% for the paint films containing 40%, 30%, 20% and 10% binder, respectively. In the case of ideal pigmentation, a decrease of water solubility in the paint film is expected when volume fraction of impermeable pigment increases (van der Wel and Adan, 1999). This observation is in agreement with the results reported in this study since the increase in volume fraction of the pigments is equivalent to the decrease in the volume fraction of the binder.

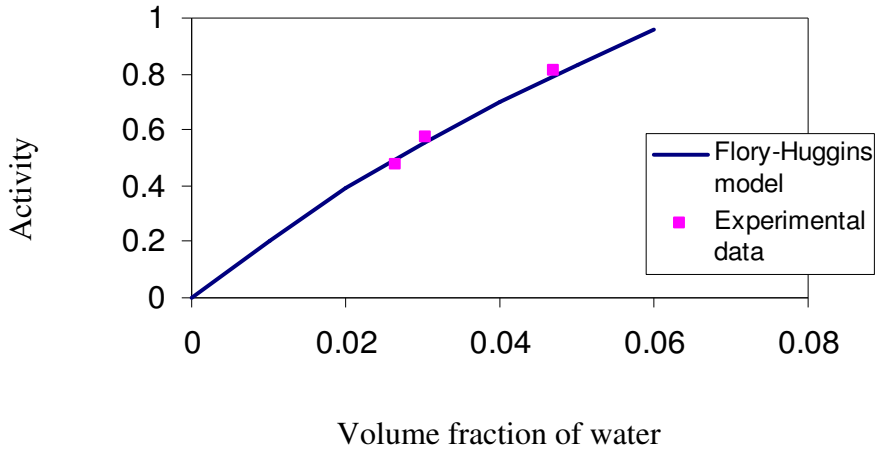

Figure 5.35: Water vapour sorption equilibria for the paint containing 40% binder at T= 30 ^{o}C.

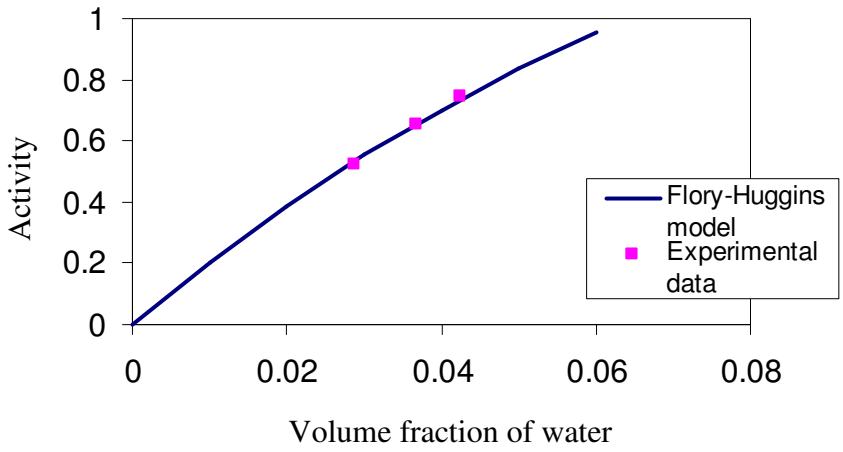

Figure 5.36: Water vapour sorption equilibria for the paint containing 30% binder at T= 30 ^{o}C.

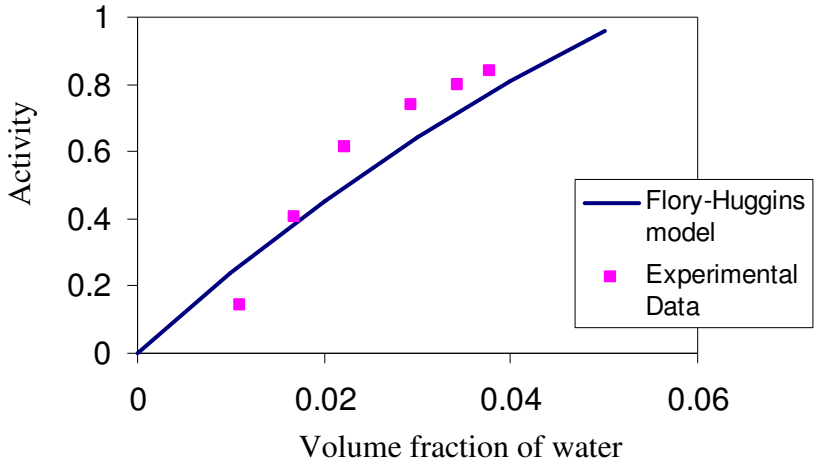

Figure 5.37: Water vapour sorption equilibria for the paint containing 20% binder at T= 30 ^{o}C.

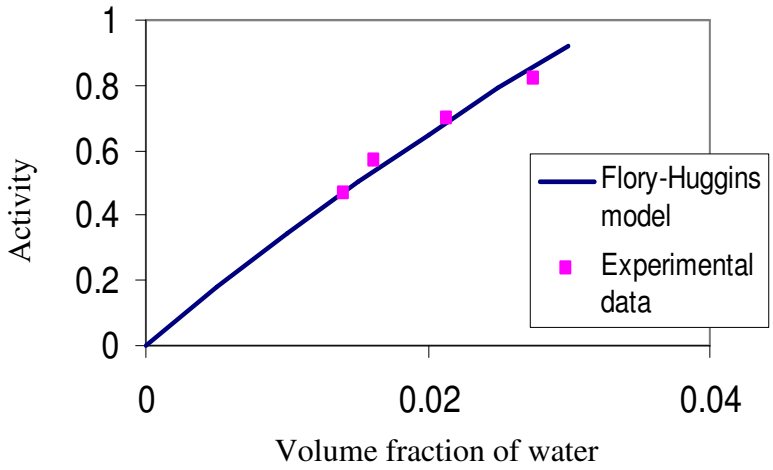

Figure 5.38: Water vapour sorption equilibria for the paint containing 10% binder at T= 30 ^{o}C.

Water vapour sorption equilibrium data in the pure copolymer is shown in Figure 5.39. It was found that the sorption isotherm for the pure copolymer does not obey the Flory-Huggins theory over the whole water activity range. At high water activities, the water sorption increases faster than that predicted by the Flory-Huggins theory. The isotherm over the whole activity range was fitted well by the ENSIC model which takes into account the possibility of cluster formation. Using the sorption data at T=30 ^{o}C and T= 40 ^{o}C, two parameters of the model were determined as k_s= 4.372 and k_p= 0.00361. Based on these values the maximum water sorption capacity of the pure

copolymer was predicted as 6.43% slightly higher than the water sorption capacity of the paint films with the binder contents of 40% and 30%.

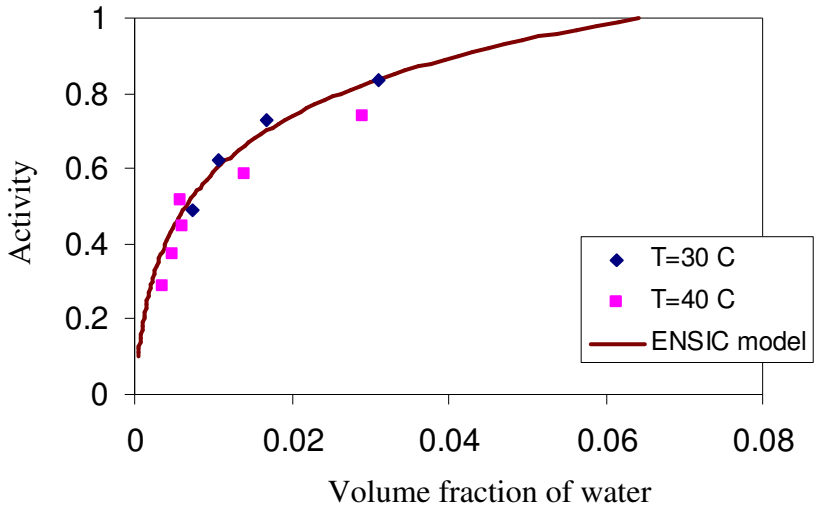

Figure 5.39: Equilibrium isotherm of the pure copolymer for T= 30 ^{o}C and 40 ^{o}C.

A significant degree of upturn in sorption data at high activities can be due to clustering of water molecules or plasticization of the polymer matrix induced by water sorption (Schult and Paul, 1996). The extend of clustering of water molecules inside the polymer matrix can be determined by the Zimm and Lundberg cluster integral (Rodriguez et al., 2003). Figure 5.40 shows the clustering function, G_{ww}/V_w as a function of water vapour activity for the pure copolymer film. For all water activities, G_{ww}/V_w values are much greater than zero indicating that water molecules tend to cluster. Figure 5.41 shows the variation of mean cluster size (MCS) as a function of the volume fraction of water in the pure copolymer. The mean cluster size defines the mean number of water molecules in excess of the mean water concentration in the neighbourhood of a given water molecule (Rodriguez et al., 2003). The large increase in the MCS with the volume fraction of water also shows a strong tendency for water to form cluster in the pure copolymer. Infact, large value of k_s (k_s= 4.372) compared to k_p value (k_p= 0.00361) indicates that mutual interactions between water molecules are much more important than the interaction between the copolymer and water molecules.

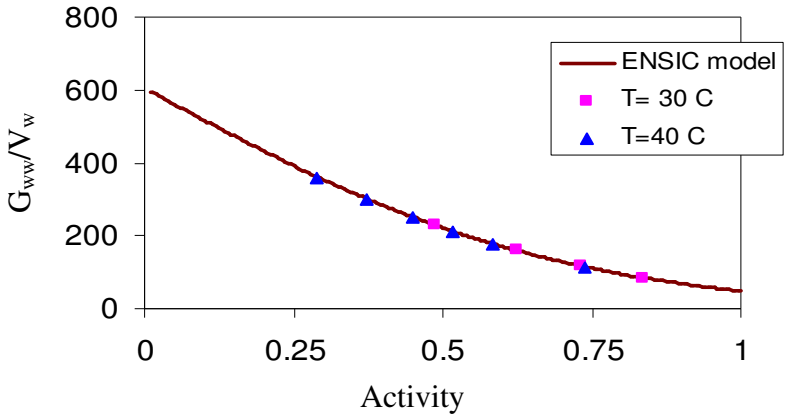

Figure 5.40: Clustering function as a function of water vapour activity for the pure copolymer film.

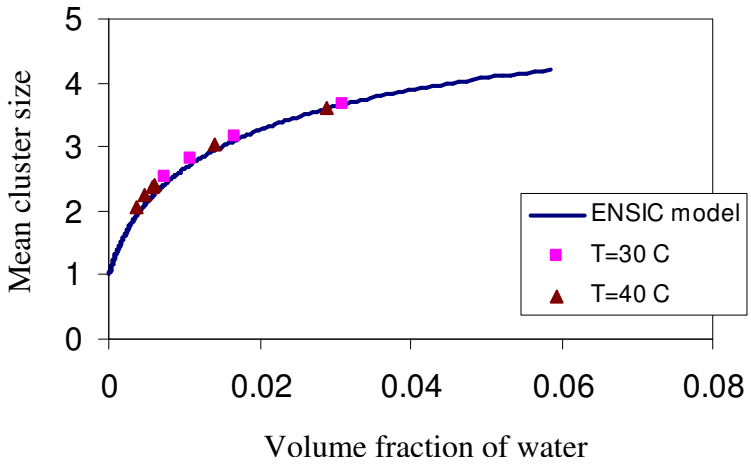

Figure 5.41: Mean cluster size as a function of the volume fraction of water in the pure copolymer film.

Figures 5.42 through 5.45 show that water molecules also form clusters in the paint films as indicated by positive values of G_{ww}/V_w at all water vapour activities. In addition, the extend of clustering slightly increases with decreasing binder content in the films. However, as illustrated in Figures 5.46 through 5.49, for all paint films the increase in mean cluster size with the sorption of water vapour is linear and lower than that in the pure copolymer. With decreasing binder content in the films, the mean cluster sizes decrease since maximum water sorption capacity decreases.

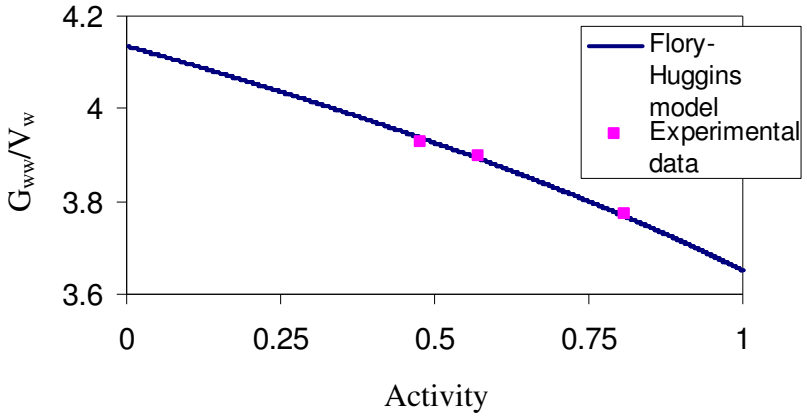

Figure 5.42: Clustering function as a function of water vapour activity for the paint film containing 40% binder.

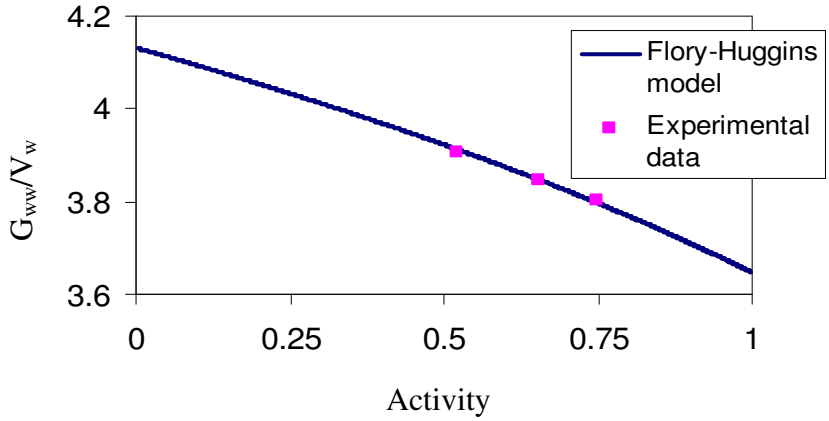

Figure 5.43: Clustering function as a function of water vapour activity for the paint film containing 30% binder.

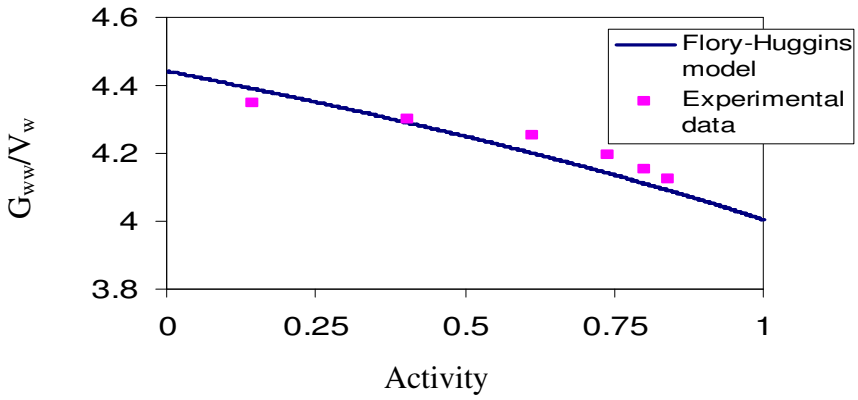

Figure 5.44: Clustering function as a function of water vapour activity for the paint film containing 20% binder.

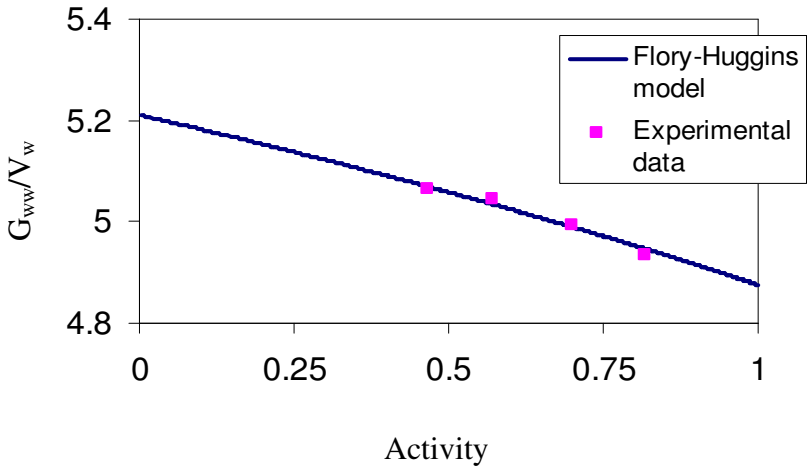

Figure 5.45: Clustering function as a function of water vapour activity for the paint film containing 10% binder.

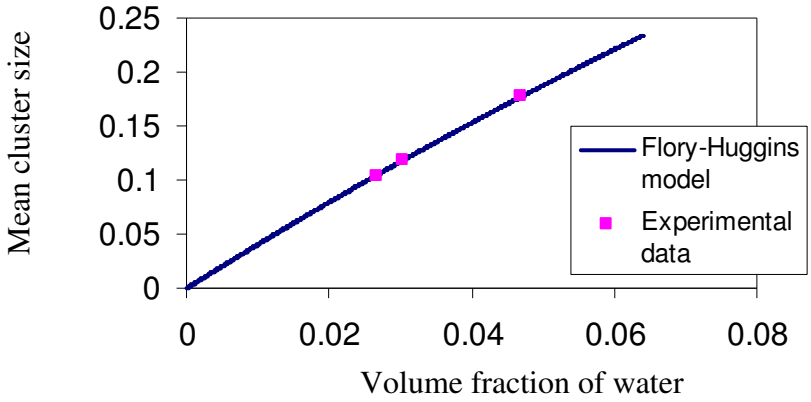

Figure 5.46: Mean cluster size as a function of the volume fraction of water in the paint film containing 40% binder.

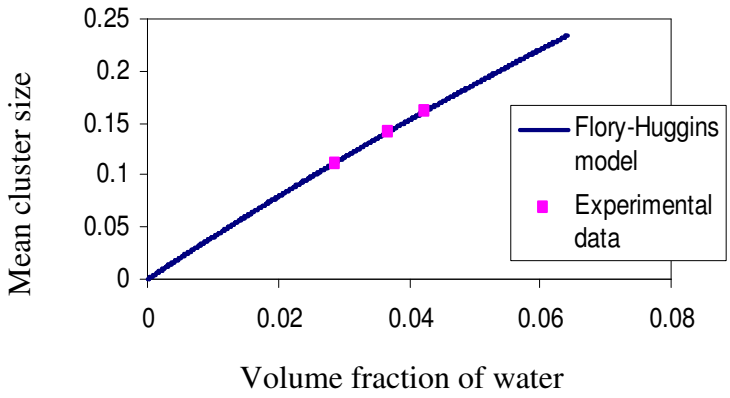

Figure 5.47: Mean cluster size as a function of the volume fraction of water in the paint film containing 30% binder.

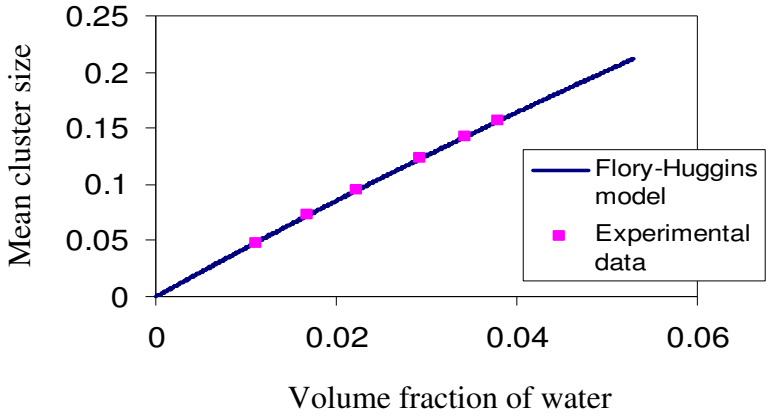

Figure 5.48: Mean cluster size as a function of the volume fraction of water in the paint film containing 20% binder.

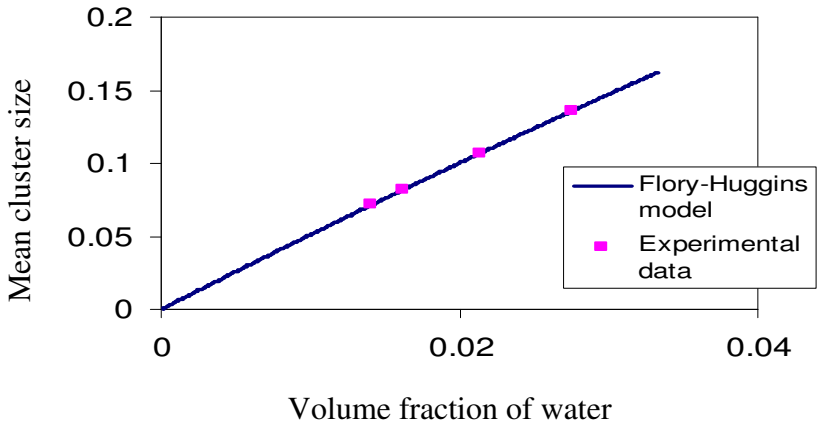

Figure 5.49: Mean cluster size as a function of the volume fraction of water in the paint film containing 10% binder.

The tendency of water molecules to form clusters in the pure copolymer and the paint films indicates that the water is not a good solvent for both pure copolymer and the paint films and the copolymer –water interaction is weak.

5.5 Diffusion Studies

5.5.1 Diffusion Studies with Paint Films

Diffusion coefficients of water in the paint films were determined at T=30 ^{o}C using magnetic suspension balance. For this purpose, normalized mass uptakes of the

films, $\frac{M_t - M_o}{M_\infty - M_o}$ were drawn against the square root of time, $\sqrt{t}$, and the results are shown in Appendix A in Figures A1 through A4. In these curves, model 1 corresponds to analytical solution given by Equation 2.9, while model 2 represents the numerical model discussed in section 2.2.2. First of all, diffusivities were calculated from the analytical solution using all experimental data. In cases when data was not fitted by the analytical solution, numerical model was adapted. In these cases, perfect fit of data with model 2 indicated that diffusion coefficient within that particular activity step is not constant. The concentration dependence of diffusion coefficient of water was described by Equation 2.20 and the exponents α_1 and α_2 in this equation determined from the best fit of the data were listed in Table 5.7. α_1 and α_2 both equal to zero corresponds to constant diffusivity case (model 1). All uptake curves are concave with respect to the $\sqrt{t}$ axis and the initial region is linear. These two observations suggest that sorption kinetics of water vapour in the paint films may follow Fickian sorption.

Table 5.7 Parameters α_1 and α_2 in Equation 2.20 for varying water concentrations in paint films.

% Binder	T (^oC)	$\omega_{average}$	α_1	α_2
40	30	0.009	0.01	450
40	30	0.014	0	0
40	30	0.021	0	0
30	30	0.009	0.01	400
30	30	0.017	0.05	700
30	30	0.019	0	0
20	30	0.004	0.01	800
20	30	0.009	0.01	2000
20	30	0.012	0.01	2000
20	30	0.015	0.01	1500
10	30	0.006	0.01	770
10	30	0.001	0.05	3000
10	30	0.012	0.01	1900

The diffusivities of water in the paint films are listed in Tables 5.8 through 5.11. These values correspond to the average weight fraction of water calculated by Equation 5.4 (Hong et al., 1998).

$$\omega_{average} = \omega_{initial} + 0.7(\omega_{equilibrium} - \omega_{initial}) \quad (5.4)$$

Table 5.8: Diffusivity data for water - paint system containing 40% binder at 30 °C.

$L_{initial}$ (μm)	$P_{solvent}$ (Pa)	$\omega_{initial}$	$\omega_{equilibrium}$	$Dx10^7$ (cm^2/s)
37.3	2075	0	0.013	0.39
38.3	2500	0.013	0.015	1.5
38.5	3500	0.016	0.024	2.9

Table 5.9: Diffusivity data for water - paint system containing 30% binder at 30 °C.

$L_{initial}$ (μm)	$P_{solvent}$ (Pa)	$\omega_{initial}$	$\omega_{equilibrium}$	$Dx10^7$ (cm^2/s)
66	2280	0	0.014	1.27
68	2860	0.014	0.018	1.87
69	3260	0.018	0.021	10

Table 5.10: Diffusivity data for water - paint system containing 20% binder at 30 °C.

$L_{initial}$ (μm)	$P_{solvent}$ (Pa)	$\omega_{initial}$	$\omega_{equilibrium}$	$Dx10^6$ (cm^2/s)
121	580	0	0.006	3.17
122	1630	0.006	0.009	2.02
123	2500	0.009	0.013	1.78
124	3000	0.013	0.017	1.5

Table 5.11: Diffusivity data for water - paint system containing 10% binder at 30 °C.

$L_{initial}$ (μm)	$P_{solvent}$ (Pa)	$\omega_{initial}$	$\omega_{equilibrium}$	$Dx10^6$(cm^2/s)
130	1970	0	0.009	3.06
132	2400	0.009	0.01	1.7
133	2950	0.01	0.013	0.99

Figure 5.50 plots diffusivities of all paint films as a function of average weight fraction of water. The diffusion coefficient of water increases with decreasing binder fraction in the paint. This was an expected result since paint structure changes from an

almost nonporous to porous one as the binder amount decreases from 40% to 10% as shown by the SEM pictures in Figure 5.9.

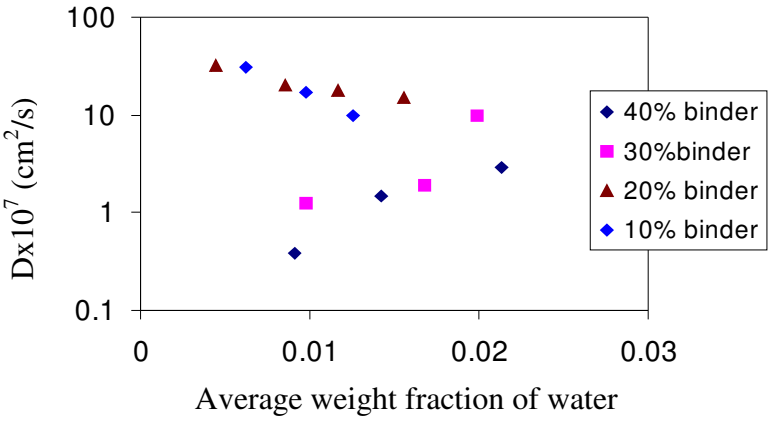

Figure 5.50: Diffusion coefficient of water in the paint films as a function of its average weight fraction at T=30 ^{o}C.

In paint films containing 20% and 10% binder, amount of binder is not sufficient to wet the pigments, thus pigment flocculation and consequently pore formation is clearly observed in these films, facilitating water transport. For paint films containing 20% and 10% binder, diffusivity decreases slightly while for the paint film containing 30% binder it increases almost one order of magnitude with increasing weight fraction of water in the film. A slight increase in diffusivity with increasing water content was observed for the paint film containing 40% binder. The increase in diffusion coefficient is associated with the plasticization of the binder by the water, while the decrease in diffusivity is due to clustering of water molecules. The results suggest that when the binder fraction of the paint film is low (20% and 10% respectively), clustering is dominant, thus diffusivity decreases. For the paint films containing 40% and 30% binder, plasticization effect is dominant over the whole activity range, consequently, diffusivity increases.

Perez et al. (1999) determined the diffusion coefficient of water in a water-borne acrylic paint as 0.71×10^{-7} cm^2/sec which has the same order of magnitude for the paint film containing 40% binder.

5.5.2 Diffusion Studies with Pure Copolymer Film

Diffusion coefficient of water in the pure copolymer film was determined at 30 ^{o}C and 40 ^{o}C. Experimental mass uptake curves are given in Figures A5 through A6. Experimental data collected at 40 ^{o}C were all fitted well by the Crank's analytical solution (model 1) except the last activity step. However, deviation from the analytical solution was observed in evaluating the data at 30 ^{o}C, thus diffusivities in these cases were determined from the numerical model (model 2). The constants α_1 and α_2 determined from the fit of numerical model to the data are listed in Table 5.12 and 5.13. Water sorption in pure copolymer also follows Fickian diffusion since all uptake curves are concave to the $\sqrt{t}$ axis and their initial initial regions are linear. The diffusivities at 30 ^{o}C and 40 ^{o}C corresponding to average weight fraction of water in the copolymer are listed in Tables 5.14 and 5.15, respectively and diffusion coefficient values as a function of average weight fraction of water was represented in Figure 5.51.

The diffusivity increases with rising temperature due to an increase in mobility of water molecules. At each temperature, plasticization effect of water molecules is dominant at low activities, thus diffusivity increases and reaches to a maximum after which clustering of water molecules becomes more important, consequently, diffusivity decreases. The increase in diffusivity associated with the plasticization effect is due to increased segmental polymer mobility caused by water molecules. On the other hand, when water molecules form cluster its effective diameter increases, which decreases mobility of the water molecules or the diffusion coefficient.

For pure copolymer films, the dominant effect of clustering at high activities is an expected result since the large increase in mean cluster size with the sorption was observed as shown in Figure 5.41.

Table 5.12: Parameters α_1 and α_2 in Equation 2.20 for varying water concentrations in pure copolymer film for T= 30 ^{o}C.

$\omega_{average}$	α_1	α_2
0.005	0.05	700
0.009	0	0
0.025	0.05	300

Table 5.13: Parameters α_1 and α_2 in Equation 2.20 for varying water concentrations in pure copolymer film for T= 40 °C.

ω average	α_1	α_2
0.002	0	0
0.004	0	0
0.005	0	0
0.007	0	0
0.012	0	0
0.023	0.05	250

Diffusivities of water in the pure copolymer film at T= 30 °C are close to the values determined in the paint film containing 40% binder. This result is consistent with those of sorption and permeation studies. Specifically, permeability and maximum water sorption capacity of the pure copolymer are close to the values determined for the paint film with the binder content of 40%.

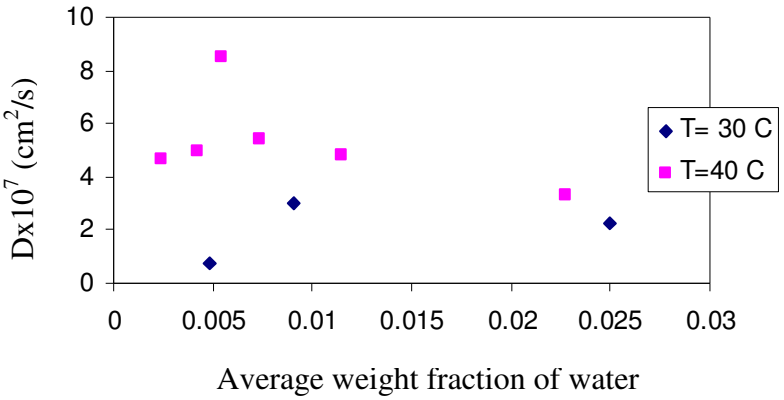

Figure 5.51: Diffusion coefficient of water in the pure copolymer as a function of its average weight fraction at 30 °C and 40 °C.

Table 5.14: Diffusivity data for water- pure copolymer system at T= 30 °C

$L_{initial}$ (µm)	$P_{solvent}$ (Pa)	$\omega_{initial}$	$\omega_{equilibrium}$	$Dx10^7(cm^2/s)$
80	2040	0	0.007	0.75
80.6	2620	0.007	0.010	3
82.1	3500	0.016	0.029	2.24

Table 5.15: Diffusivity data for water- pure copolymer system at T= 40 ^{o}C

$L_{initial}$ (μm)	$P_{solvent}$ (Pa)	$\omega_{initial}$	$\omega_{equilibrium}$	$Dx10^{7}$(cm^{2}/s)
80	2040	0	0.0034	4.68
80.3	2620	0.0034	0.0046	4.93
80.4	3160	0.0046	0.0058	8.50
80.5	3640	0.0058	0.008	5.44
80.7	4120	0.008	0.013	4.80
81.1	5200	0.013	0.027	3.34

CONCLUSIONS AND SUGGESTIONS FOR FUTURE WORK

In this study, transport properties (permeability, solubility, diffusivity) of water in water borne acrylic based paint and in methylmethacrylate-co-butylacrylate copolymer used as a binder in the paint were measured. Furthermore, the structure of the paint films which have the same formulation but differ in binder amount as 40%, 30%, 20% and 10% was determined using different characterization tools.

Paint samples were supplied by Akril Kimya A.Ş. and no information was provided about the paint ingredients and their compositions except the composition of the binder. Energy dispersive X-Ray (EDX) analysis allowed to determine common elements in all paint films which can be listed as carbon, oxygen, calcium, titanium, silicon, magnesium, aluminium, and sodium. According to the X-ray analysis, titanium element in the paint is found as titania while calcium is in the form of calcite both of which are mostly used as pigment and filler material in the paint formulations. Scanning electron microscope pictures have shown that as the amount of binder decreases from 40% to 10%, the structure of the films changes from almost nonporous to a porous one. Porous structure formation is a result of the pigment flocculation due to insufficient wetting of pigments by the binder. Map diagrams of the paint films have shown that in paint films with low contents of binder (20%, 10%) distribution of the pigments is not homogeneous. Thermal gravimetric analysis indicated that pure copolymer degrades at one step without leaving a thermally stable char, while paint films decompose at two steps leaving thermally stable char which contains CaO and titania which are both stable above 1000 ^{o}C. Based on differential scanning calorimetry analysis, it was observed that the pure copolymer exhibits one endothermic decompositon peak while paint films exhibit two exothermic decomposition peaks. Glass transition temperature of the pure copolymer (T_g= 31.67 ^{o}C) was found to be slightly lower than those of the paint films (34.1 ^{o}C, 34.1 ^{o}C, 32.8 ^{o}C, 33.9 ^{o}C for the paint films in the order of decreasing binder amount). Solid content of the paint films (%) increases from 72% to 75% as the amount of binder decreases from 40% to 10%.

Sorption data when presented by plots of $\frac{M_t - M_o}{M_\infty - M_o}$ as a function of $\sqrt{t}$ have shown that sorption kinetics for both the paint films and the pure copolymer film may

be classified as Fickian type since the initial regions of the curves are linear and are always concave with respect to axis above the linear portion. Diffusivities were determined by fitting either the analytical or numerical model to the sorption data. Diffusivities increase with increasing water content of the films due to plasticization effect of water, while they tend to decrease when water molecules form clusters. Predictions have shown that water form clusters both in the paint films and in the pure copolymer. Degree of clustering and the change of mean cluster size with sorption appears to be larger for the pure copolymer.

Diffusivity of water increases with decreasing binder fraction in the paint film. This is due to pore formation and nonhomogeneous distribution of the pigments in the paint films with low binder content.

Vapour-sorption equilibrium data were fitted by the Flory-Huggins theory and ENSIC model for the paint films and the pure copolymer, respectively. Predictions from these theories have shown that maximum water sorption capacity of the paint films decreases with decreasing binder fraction in the paint film. Permeability coefficient of water also increases as the amount of binder in the paint film decreases. Maximum water sorption capacity, diffusivity and permeability of water in the paint film containing 40% binder are similar to the corresponding values determined for the pure copolymer film. This result suggests that the paint sample containing 40% binder shows the best barrier property against water.

Combined with the characterization studies, it can be concluded that binder fraction in the paint is important since it directly influences the homogeneous distribution, flocculation of the pigments and pore formation in the structure, consequently, the water transport and the barrier property of the paints.

Future work should involve the measurement of diffusivity and solubility of monomers of the binder (methylmethacrylate and butylacrylate) and the atmospheric gases (O_2, N_2) in the paint films. The former data are required to predict the emission of these monomers from the paint while the latter data are required to further determine the barrier property of the paint when it is applied on outdoor surfaces.

REFERENCES

Adan O.C.G, van der Wel G.K, Moisture in organic coatings-a review, *Progress in Organic Coatings*, **37**, (1999), 1.

Alsoy S, Duda J.L, Influence of swelling and diffusion-induced convection on polymer sorption processes, *A.I.CHE. J*, **48**, (2002), 1849.

Barbucci A, Delucchi M., Goretta. L., Cerisola G, Electrochemical and physico-chemical characterization of flourinated organic coatings for steel and concrete protection: influence of pigment volume concentration, *Progress in Organic Coatings*, **33**, (1998),139.

Barrie J.A, Water in polymers, In *Diffusion in Polymers*, Edited by J. Crank and G.S. Park (Academic Press, London, 1968).

Bierwagen G.P, The science of durability of organic coatings: a foreword, *Progress in Organic Coatings*, **15**, (1987), 179.

Brisson A, Haber A, Factors affecting titanium dioxide dispersion in trade sales paints, *Journal of Coating Technology*, **63**, (1991), 59.

Brown R.G.F, Carr C, Taylor M.E, Effect of pigment volume concentration and latex particle size on pigment distribution, *Progress in Organic Coatings*, **30**, (1997),185.

Burgos M, Langlet M, The sol-gel transformation of TIPT coatings: a FTIR study, *Thin Solid Films*, **349**, (1999),19.

Cannon L.A, Pethrick R.A, Comparison of the effect of reactive and non-reactive steric stabilisers on the mechanism of film formation in methyl methacrylate/butyl acrylate copolymer latexes. part 1. differential scanning calorimetry, dynamic mechanical analysis and atomic force microscopy, *Polymer*, **43**, (2002), 6421.

Corfias C, Pébere N, Lacabanne C, Characterization of a thin protective coating on galvanized steel by electrochemical impedance spectroscopy and a thermostimulated current method, *Corrosion Science*, **41**, (1999), 1539.

Colthup N.B, Daly L.H, Wiberley S.E, *Introduction to Infrared and Raman Spectroscopy*, Third ed., (Academic Press, Inc., California, 1990).

Crank J, *The Mathematics of Diffusion*, Second ed., (Oxford University Press, Oxford, 1975).

George S.C, Thomas S, Transport phenomena through polymeric systems, *Progress in Polymer Science*, **26**, (2001), 985.

Ghi P, Hill J.T.D, Whittaker K.A, Water sorption by poly(tetrahydrofurfuryl methacrylate-co-2-hydroxyethyl methacrylate) I A mass uptake study, *Journal of Polymer Science: Part B: Polymer Physics*, **38**, (2000), 1939.

Hong S.U, Laurer J.H, Zielinski J.M, Samseth J, Smith S.D, Duda J.L, Spontak R.J, Morphological and isothermal diffusive probe analyses of low molecular-weight diblock copolymers, *Macromolecules*, **31**, (1998), 2174.

Huldén M, Hansen C. M, Water permeation in coatings, *Progress in Organic Coatings*, **13**, (1985), 171.

Jeoung-Ah K, The characterisation of paper composite porcelain in a fired state by XRD and SEM, *Journal of the European Ceramic Society*, **24**, (2004), 3823.

Keddie J.L, Film formation of latex, *Materials Science and Engineering: R: Reports*, **21**, (1997), 101.

Kristoffersson A, Roncari E, Galassi C, Comparison of different binders for water-based tape casting of alumina, *Journal of the European Ceramic Society*, **18**, (1998), 2123.

Landolt D, Guillaumin V, Effect of dispersion agent on the degradation of a water borne paint on steel studied by scanning acoustic microscopy and impedance, *Corrosion Science*, **44**, (2002), 179.

Le Pen C, Lacabanne C, Pébere N, Characterisation of water-based coatings by electrochemical impedance spectroscopy, *Progress in Organic Coatings*, **46**, (2003), 77.

Liu B, Li Y, Lin H, Cao C, Effect of PVC on the diffusion behaviour of water through alkyd coatings, *Corrosion Science*, **44**, (2002), 2657.

Mamaliga I, Schabel W, Kind M, Measurements of sorption isotherms and diffusion coefficients by means of a magnetic suspension balance, *Chemical Engineering and Processing*, **43**, (2004), 753.

Paul S, *Surface Coatings: science and technology*, (John Wiley and sons, Chichester, 1985).

Perera D.Y, Effect of pigmentation on organic coating characteristics, *Progress in Organic Coatings*, **50**, (2004), 247.

Pérez C, Collazo A, Izquierdo M, Merino P, Novoa X.R, Characterisation of the barrier properties of different paint systems: Part II. Non-ideal diffusion and water uptake kinetics, *Progress in Organic Coatings*, **37**, (1999), 169.

Perrin L, Nguyen Q.T, Sacco D, Lochon P, Experimental studies and modelling of sorption and diffusion of water and alcohols in cellulose acetate, *Polymer International*, **42**, (1997), 9.

Prausnitz J.M, Lichtenthaler R.N, de Azevedo EG, *Molecular Thermodynamics of Fluid-Phase Equilibria*, Second Ed., (Prentice-Hall, Inc., New Jersey, 1986).

Reigh F.B, Adelantado G.J.V, Moreno M.M.C.M, FTIR quantitative analysis of calcium carbonate (calcite) and silica (quartz) mixtures using the constant ratio method. Application to geological samples, *Talanta*, **58**, (2002), 811.

Rodriguez O, Fornasiero F, Arce A, Radke C.J, Prausnitz J.M, Solubilities and diffusivities of water vapor in poly(methylmethacrylate), poly(2-hydroxyethylmethacrylate), poly(N-vinyl-2-pyrrolidone) and poly(acrylonitrile), *Polymer*, **44**, (2003), 6323.

Schult K.A, Paul D.R, Water sorption and transport in a series of polysulfones, *J. Polym. Sci. Part B: Polym. Phys.*, **34**, (1996), 2805.

Sönmez İ, Cebeci Y, Fundamental aspects of spherical oil agglomeration of calcite, *Colloids and Surfaces A: Physicochem. Eng. Aspects*, **225**, (2003), 111.

Tiarks F, Frechen T, Kirsch S, Leuninger J, Melan M, Pfau A, Richter F, Schuler B, Zhao C. L, Formulation effects on the distribution of pigment particles in paints, *Progress in Organic Coatings*, **48**, (2003), 140.

Weismantel G.E, *Paint Handbook*, (McGraw-Hill, Inc., Newyork, 1981).

Vitala R.I, Langlet M, Simola J, Lindén M, Rosenholm J.B, Aerosol-gel deposition of doped titania thin films, *Thin Solid Films*, **368**, (2000), 35.

APPENDIX

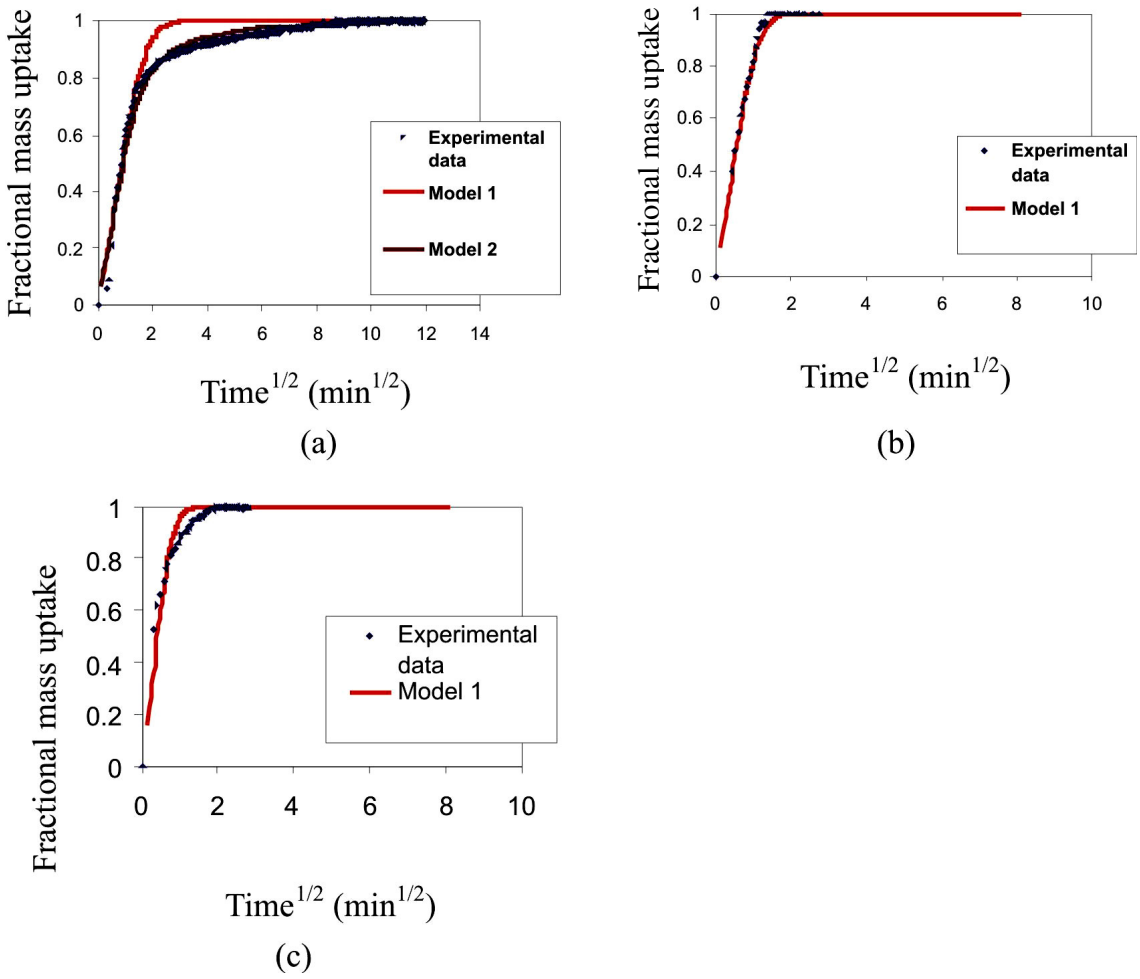

Figure A1: Fractional mass uptake curves of the paint film containing 40% binder for water vapour pressures of (a): 2075 Pa, (b):2500 Pa, (c):3500 Pa

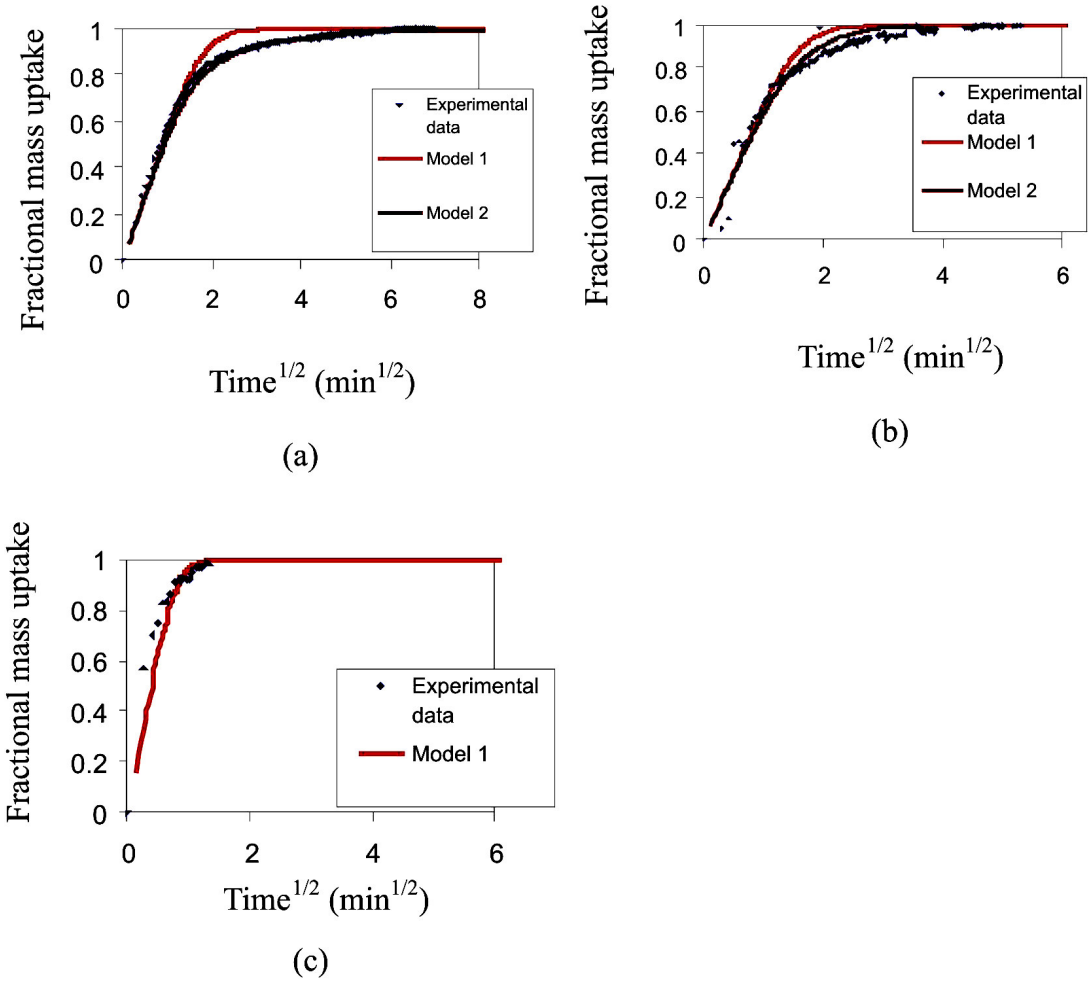

Figure A2: Fractional mass uptake curves of the paint film containing 30% binder for water vapour pressures of (a):2280 Pa, (b): 2860 Pa, (c): 3260 Pa.

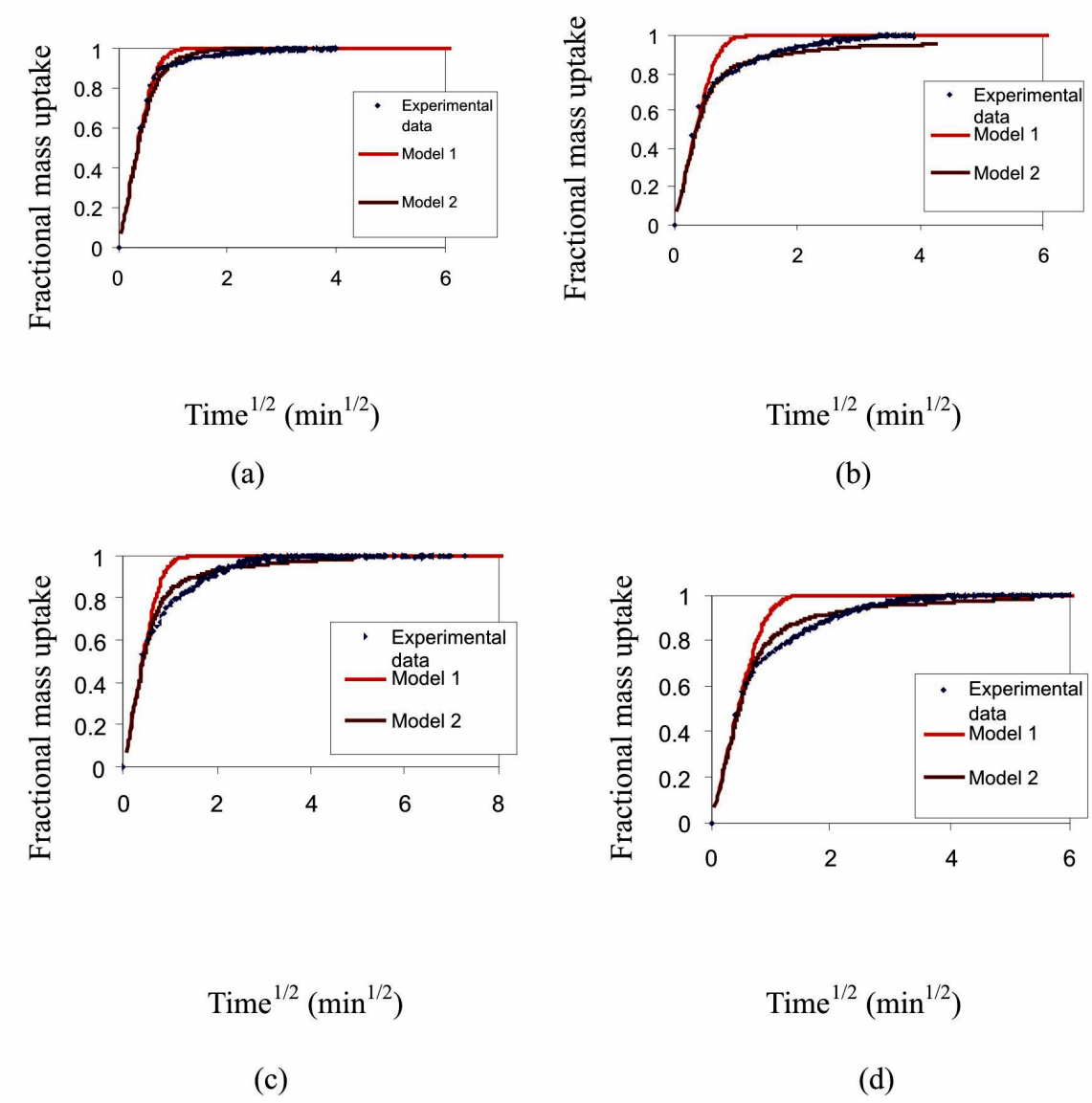

Figure A3: Fractional mass uptake curves of the paint film containing 20% binder for water vapour pressures of (a): 580 Pa, (b): 1630 Pa, (c):2500 Pa, (d): 3000 Pa.

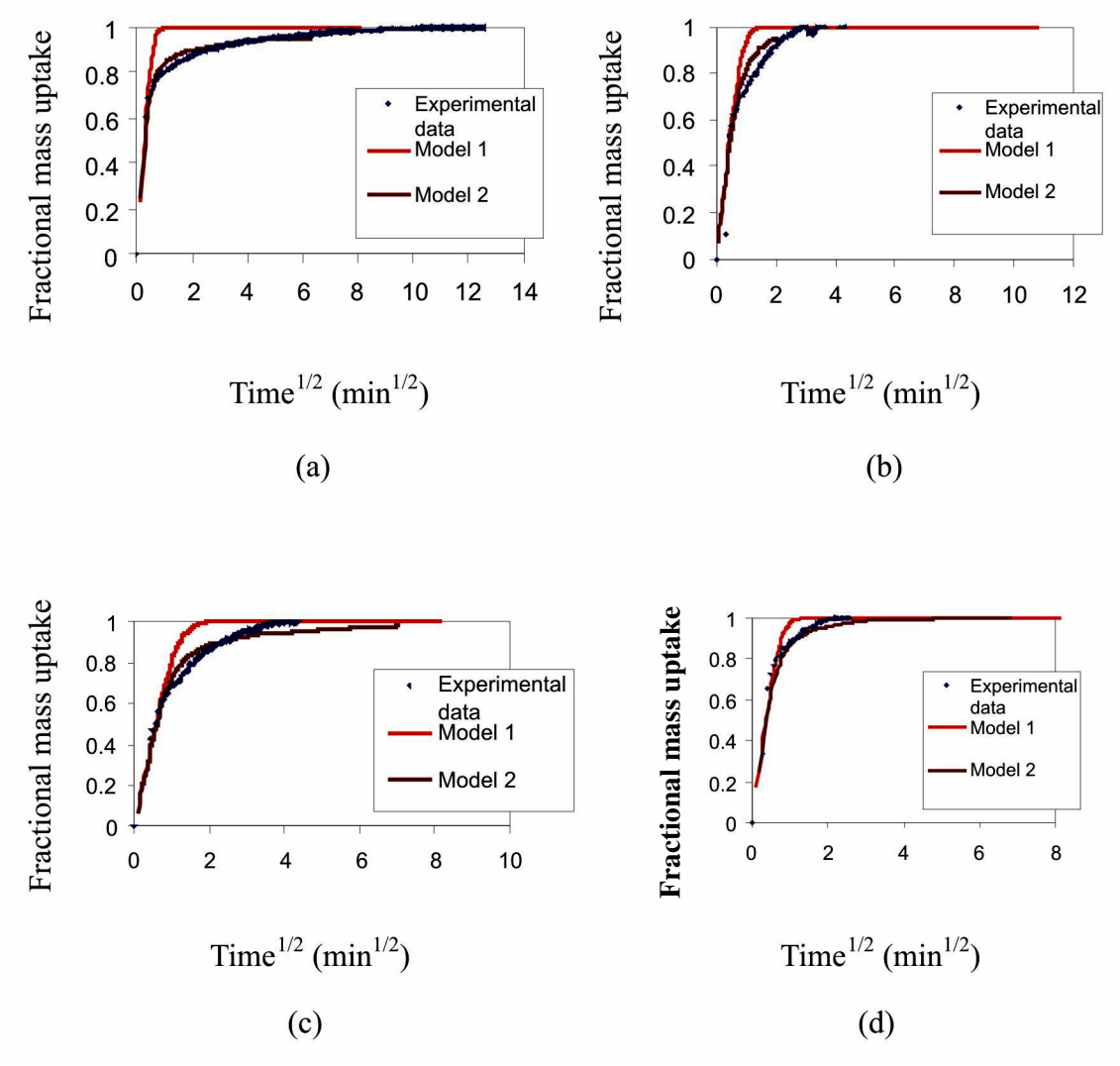

Figure A4: Fractional mass uptake curves of the paint film containing 10% binder for water vapour pressures of (a):1970 Pa, (b): 2400 Pa, (c): 2950 Pa.

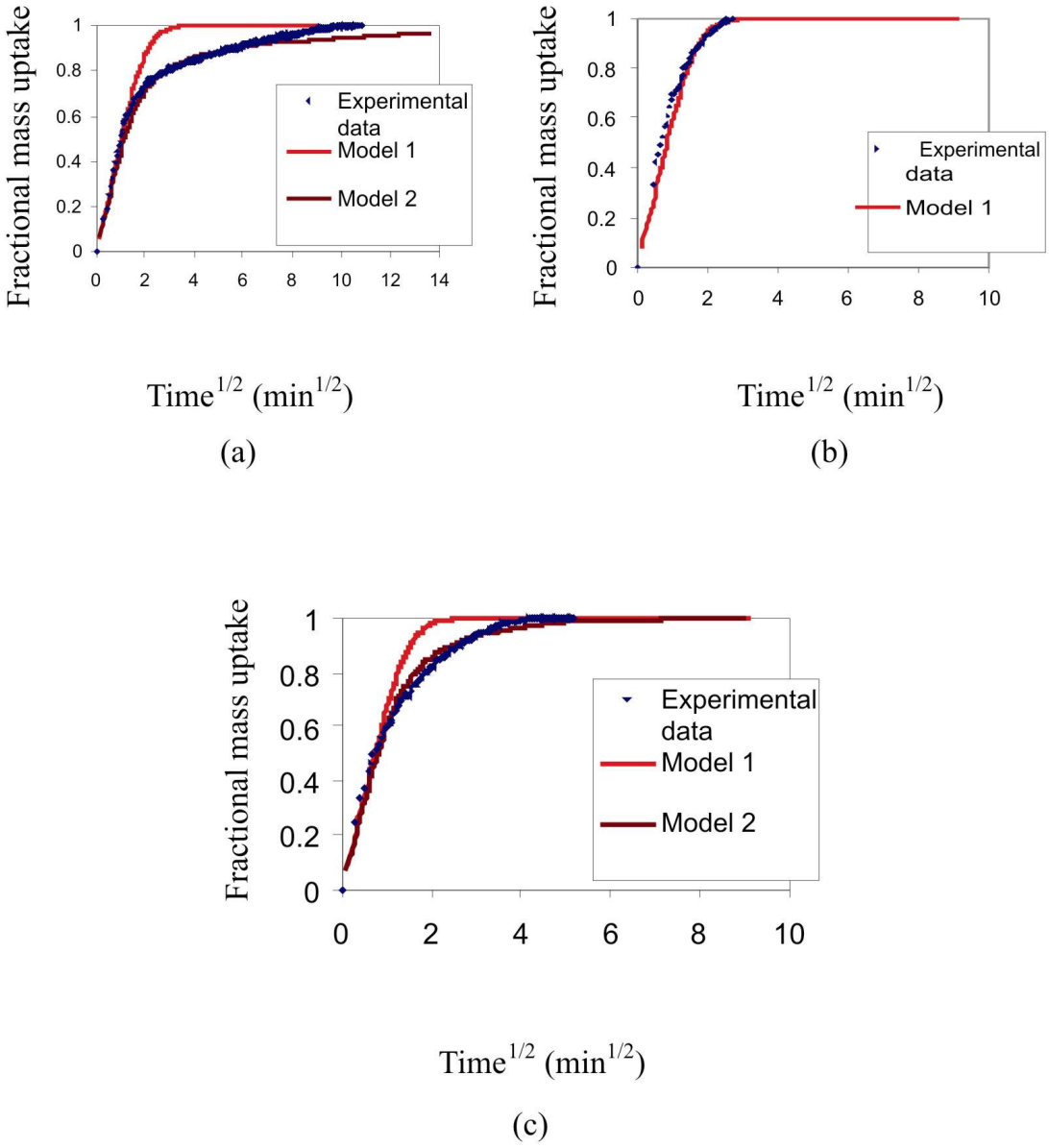

Figure A5: Fractional mass uptake curves of the pure copolymer film at T= 30 ^{o}C for water vapour pressures of (a): 2040 Pa, (b): 2620 Pa, (c): 3500 Pa.

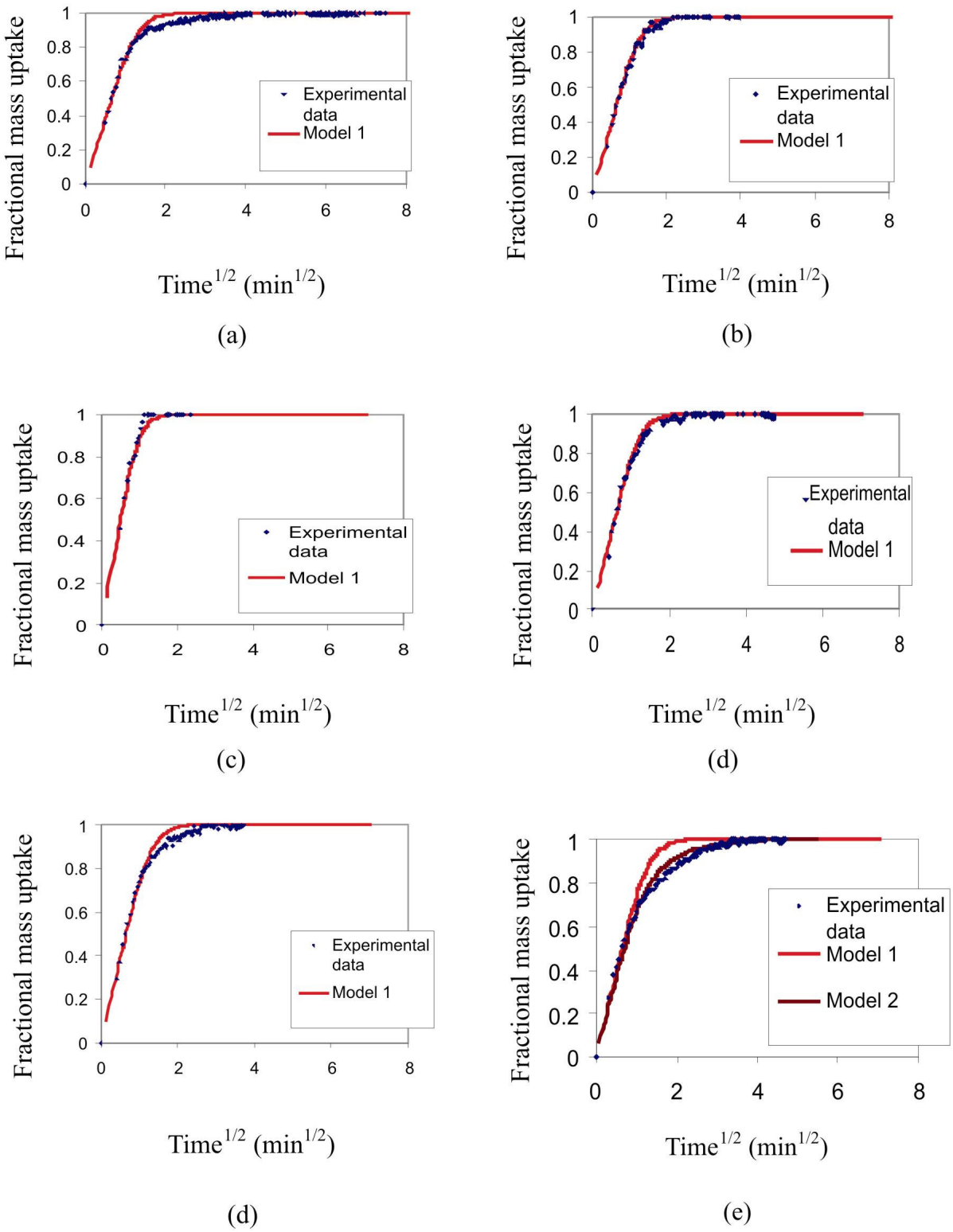

Figure A6: Fractional mass uptake curves of the pure copolymer film at T= 40 ^{o}C for water vapour pressures of (a): 2040 Pa, (b): 2620 Pa, (c): 3160 Pa, (d): 4120 Pa, (e): 5200 Pa.